

Supporting Information for

π -conjugated diimidazolium salts: rigid structures to obtain organized materials

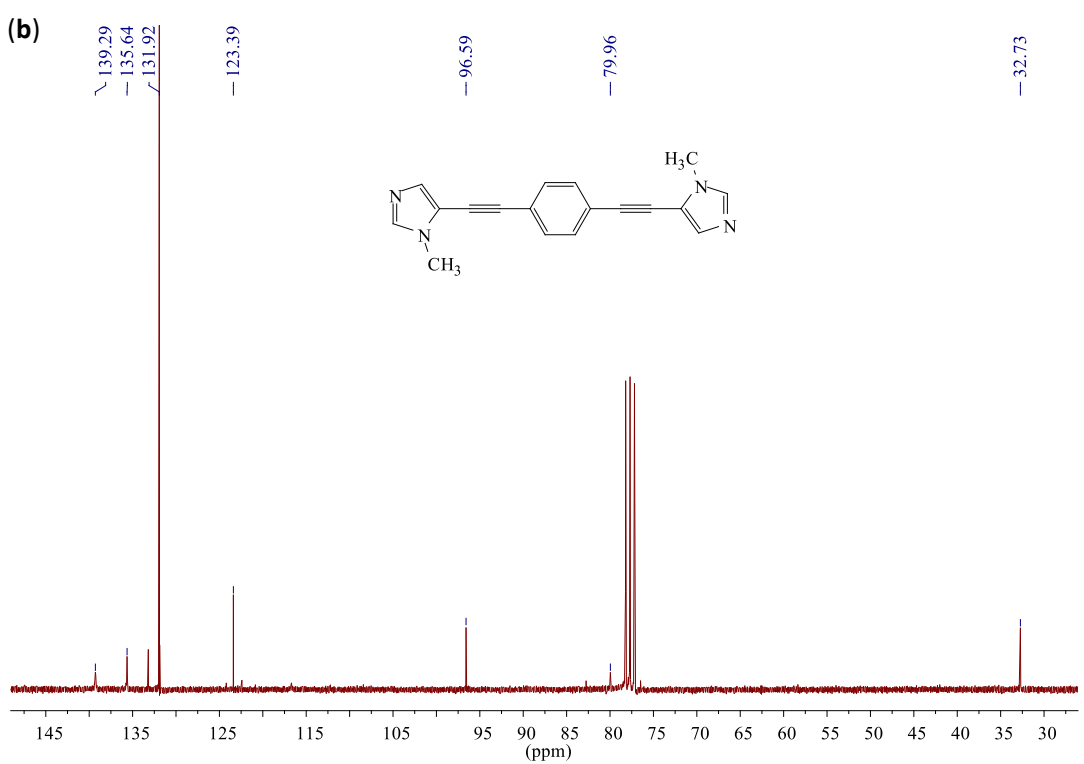
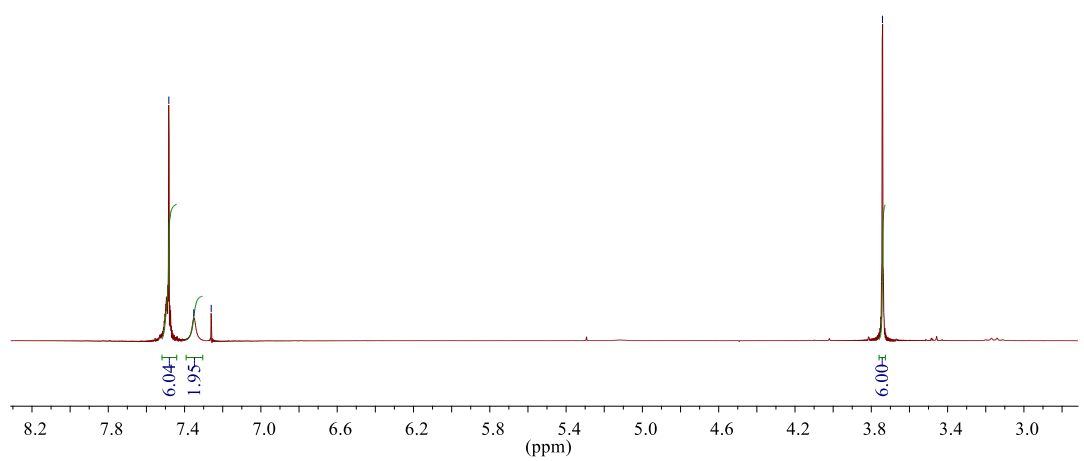
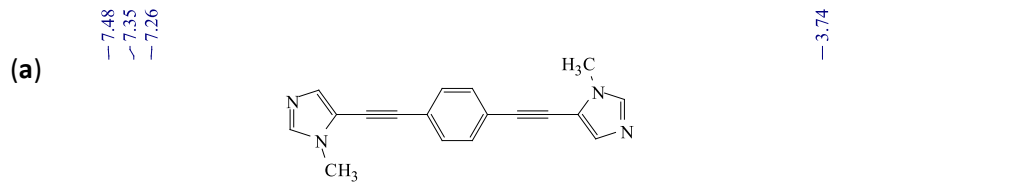
Paola Vitale,^a Francesca D'Anna,^{a} Francesco Ferrante,^b Carla Rizzo,^a Renato Noto^a*

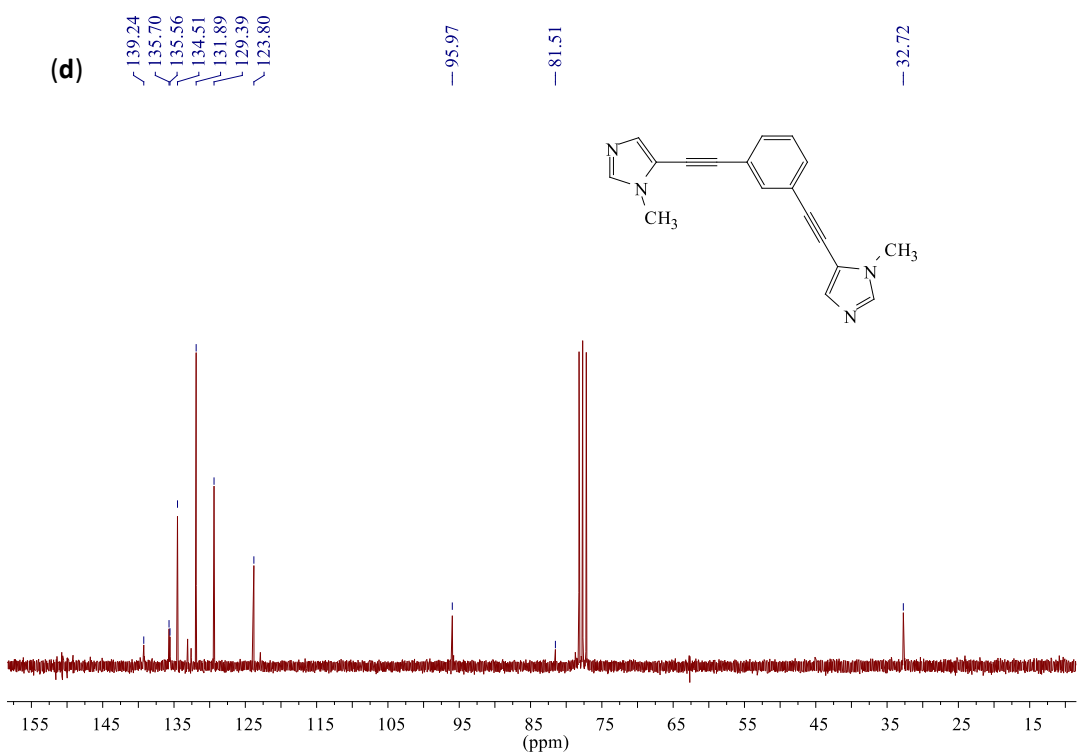
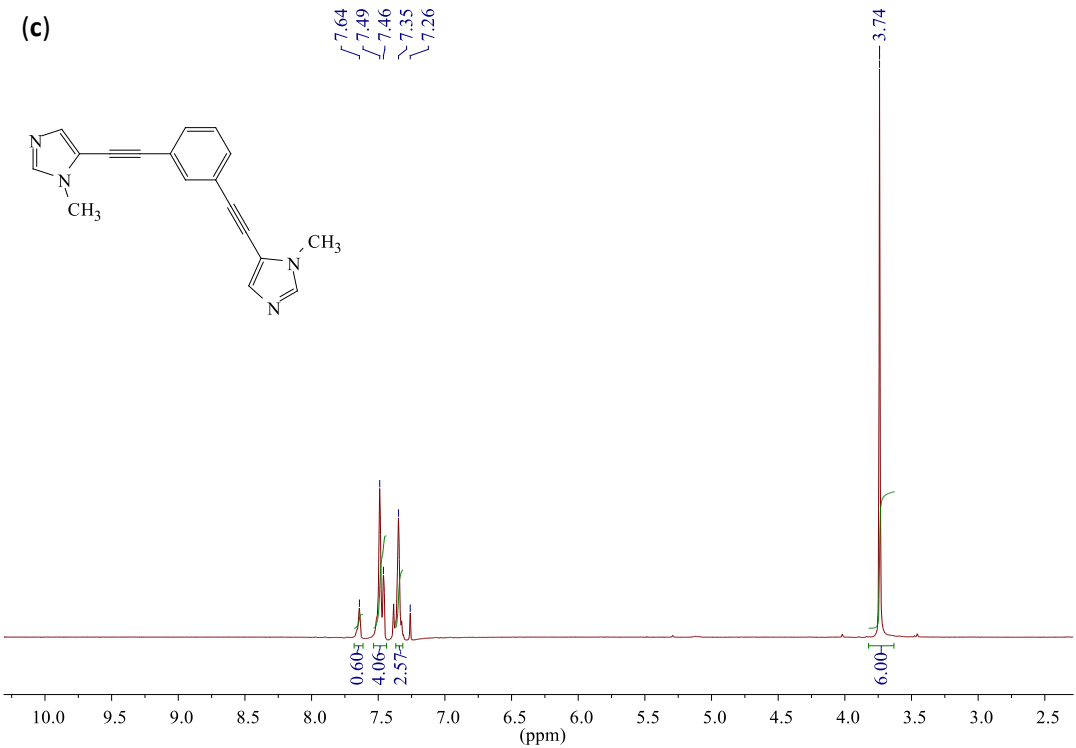
^aDipartimento STEBICEF, Università degli Studi di Palermo, Viale delle Scienze, Parco d'Orleans II, 90128 Palermo (Italy).

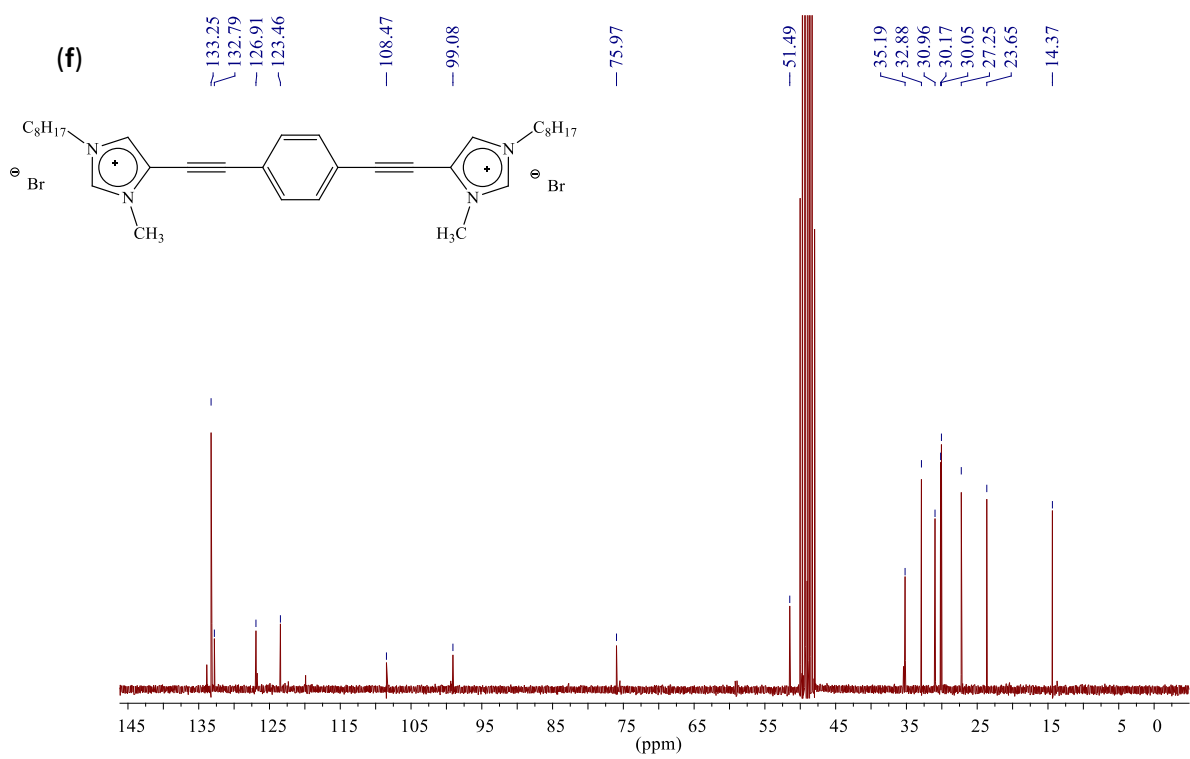
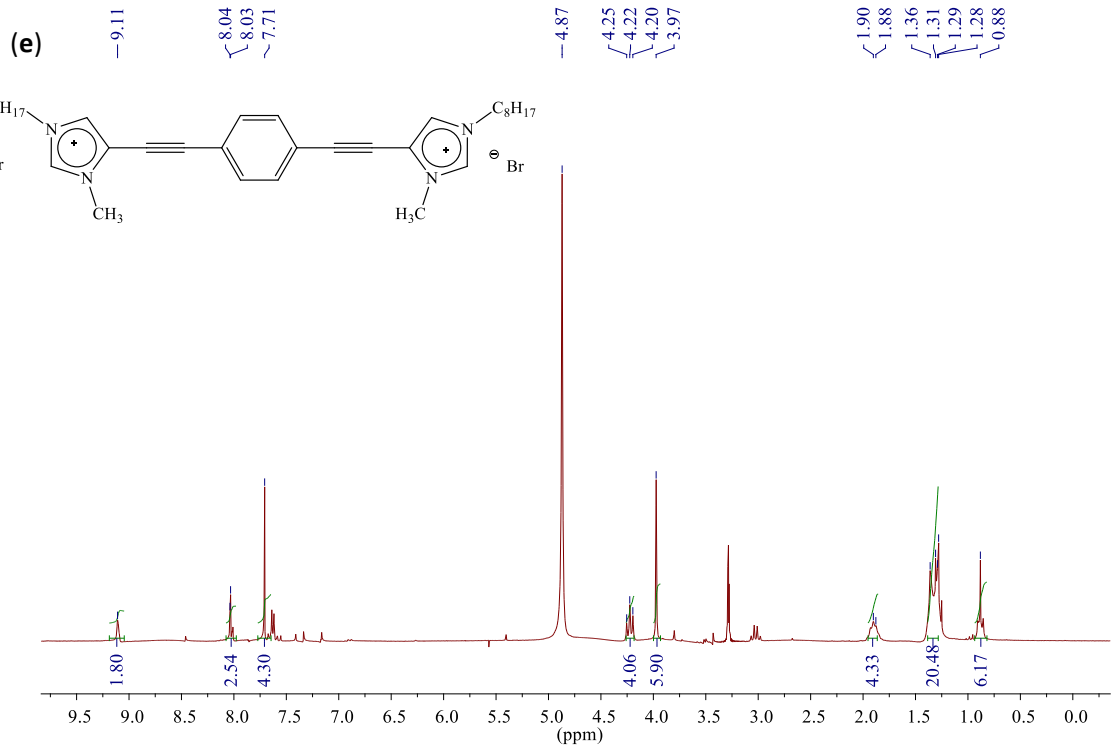
^bDipartimento di Fisica e Chimica, Università degli Studi di Palermo, Viale delle Scienze, Parco d'Orleans II, 90128 Palermo (Italy).

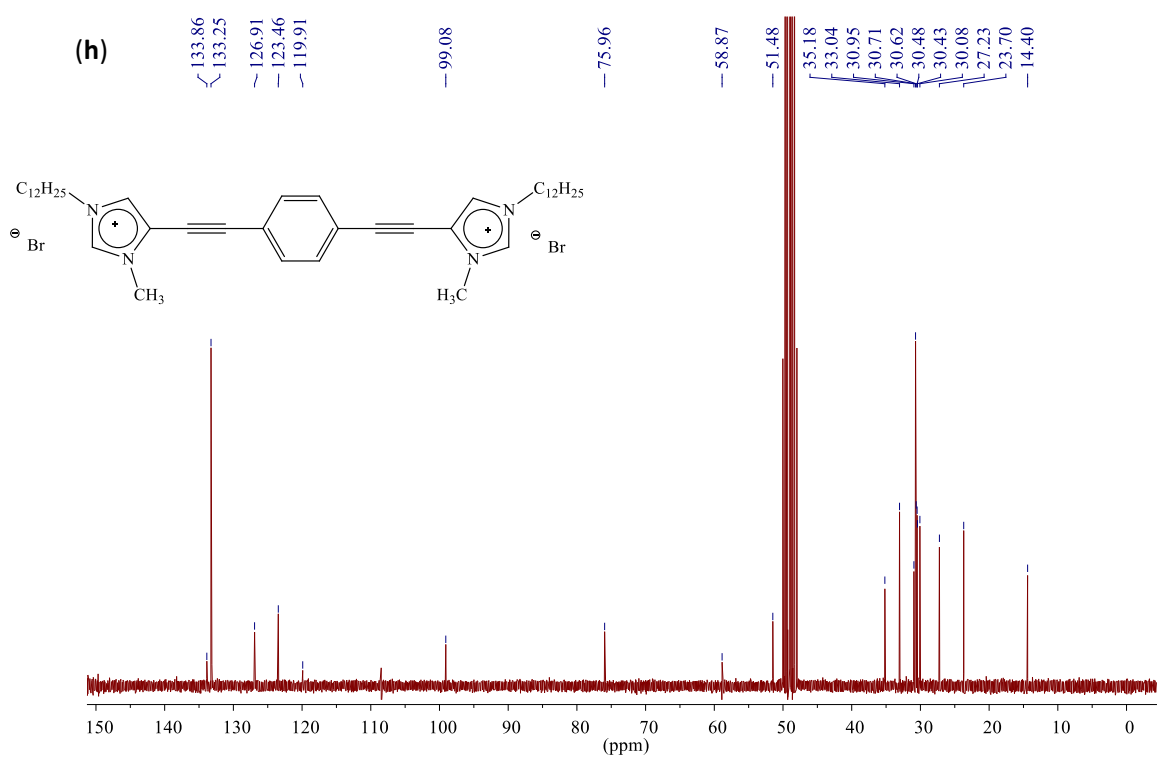
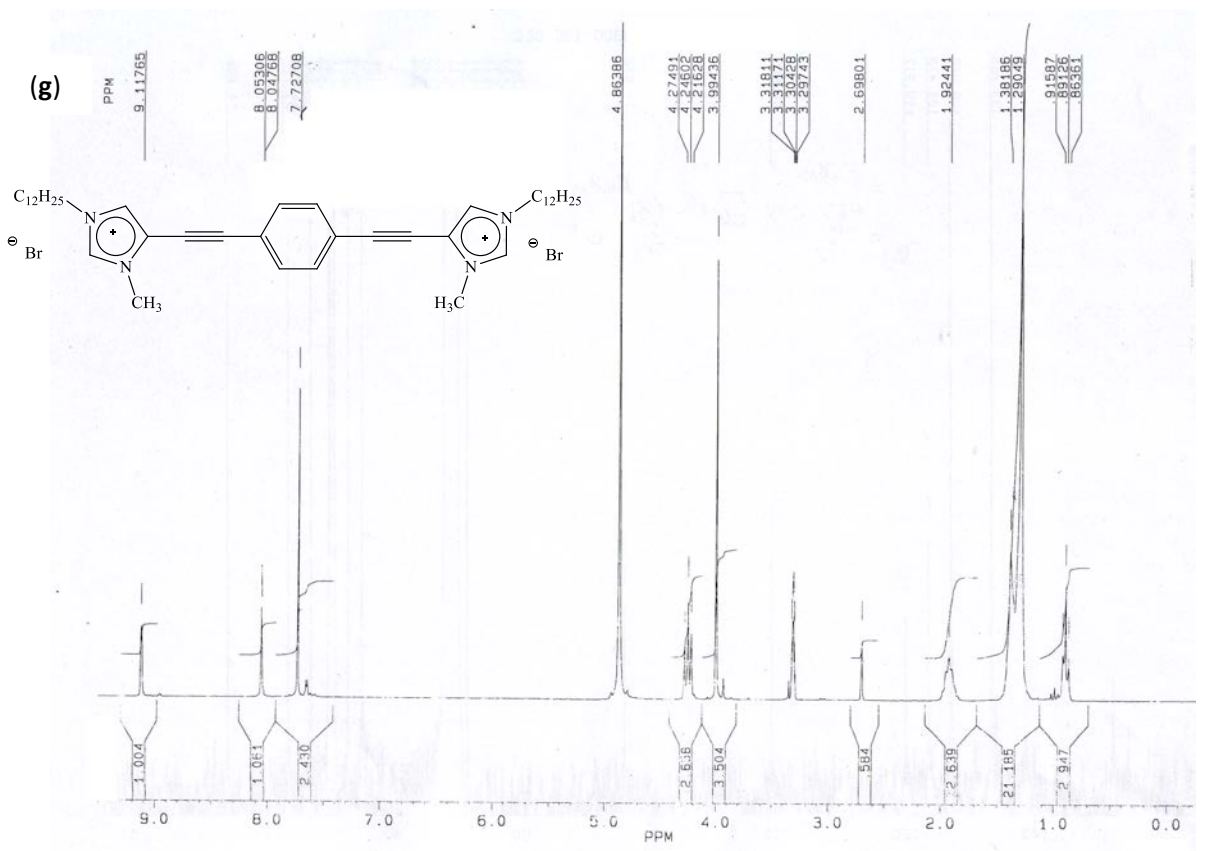
Table of Contents:

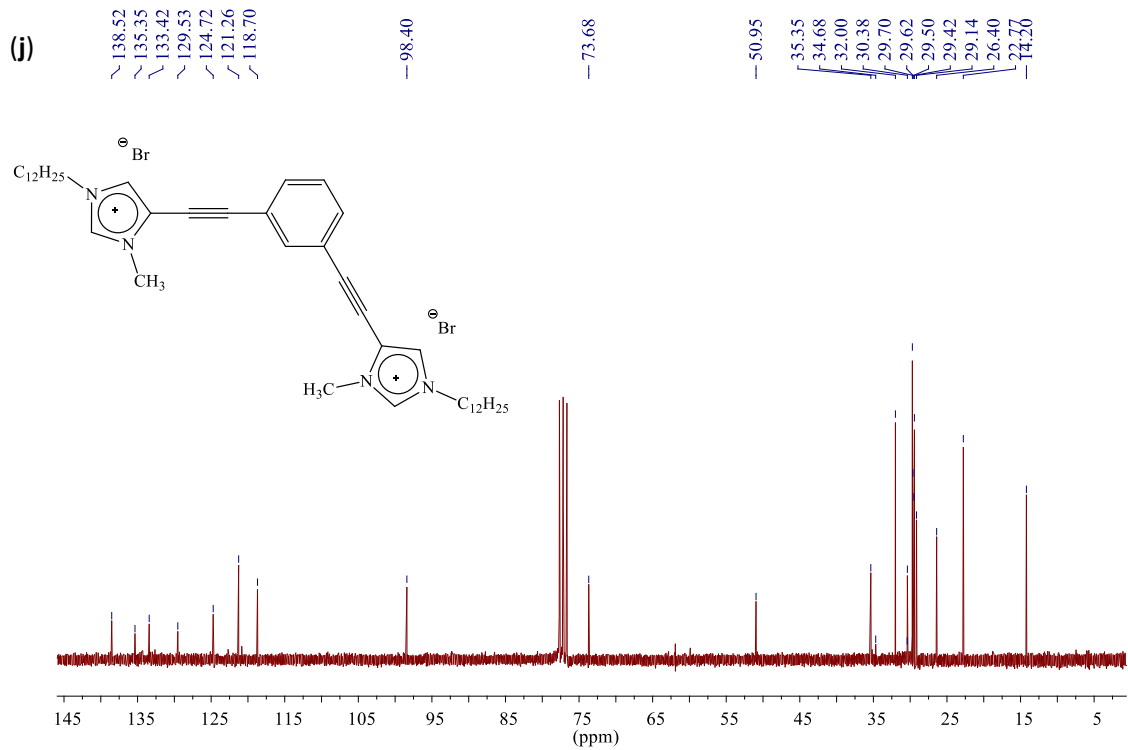
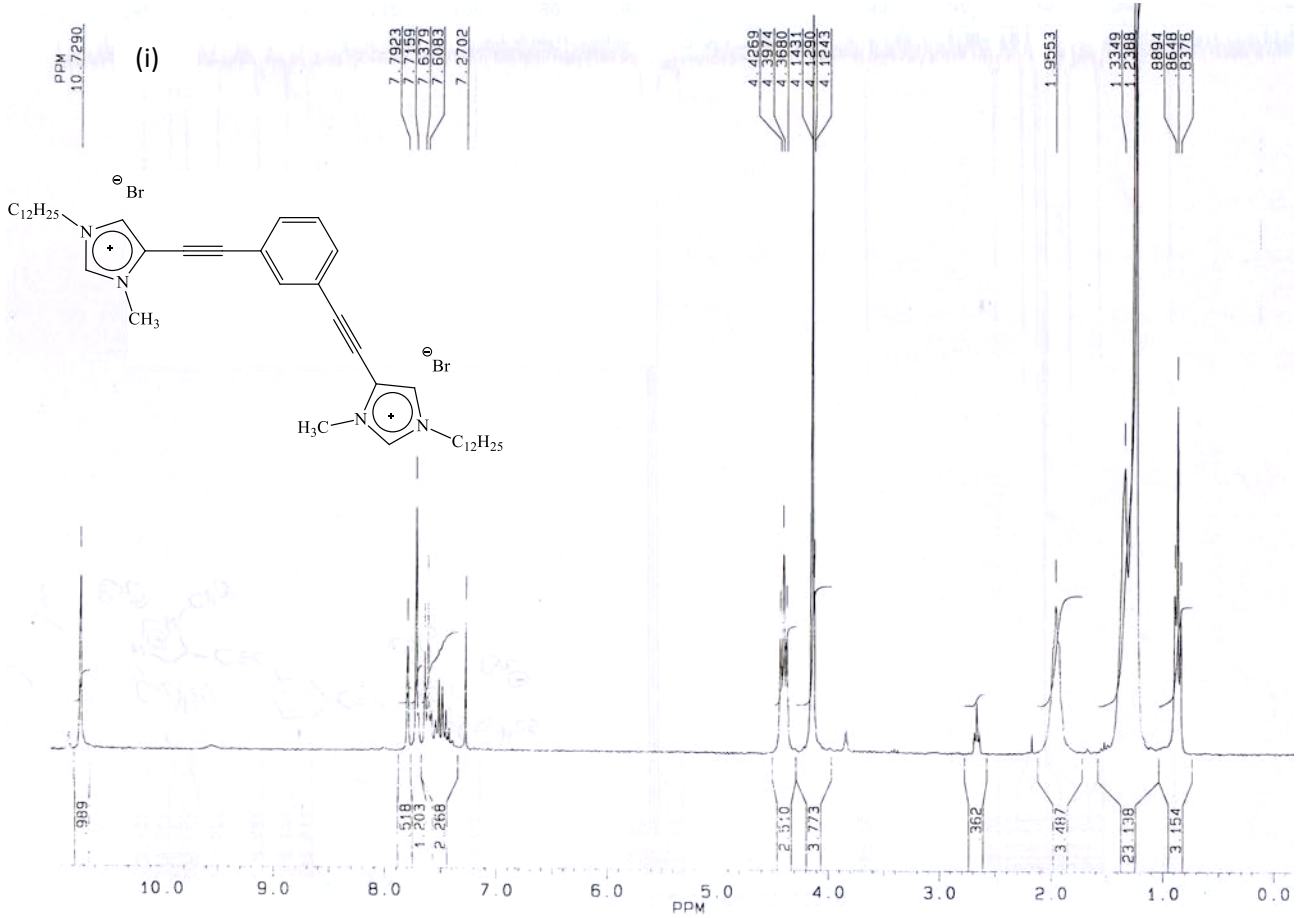
Fig. S1 ^1H NMR and ^{13}C NMR spectra corresponding to: (a), (b) 1; (c), (d) 2; (e), (f) [<i>p</i> -C ₈ Br ₂]; (g), (h) [<i>p</i> -C ₁₂ Br ₂]; (i), (j) [<i>m</i> -C ₁₂ Br ₂]; (k), (l) [<i>p</i> -C ₈ (NTf ₂) ₂]; (m), (n) [<i>p</i> -C ₁₂ (NTf ₂) ₂] and (o), (p) [<i>m</i> -C ₁₂ (NTf ₂) ₂].	S2
Fig. S2 DSC traces corresponding to: (a) 1; (b) [<i>p</i> -C ₈ Br ₂]; (c) [<i>p</i> -C ₈ (NTf ₂) ₂]; (d) [<i>p</i> -C ₁₂ Br ₂]; (e) [<i>p</i> -C ₁₂ (NTf ₂) ₂]; (f) 2; (g) [<i>m</i> -C ₁₂ Br ₂]; (h) [<i>m</i> -C ₁₂ (NTf ₂) ₂].	S10
Fig. S3 UV-vis and fluorescence spectra recorded in different solvents at 298 K for: (a) and (b) [<i>p</i> -C ₈ Br ₂]; (c) and (d) [<i>p</i> -C ₁₂ Br ₂]; (e) and (f) [<i>p</i> -C ₈ (NTf ₂) ₂]; (g) [<i>m</i> -C ₁₂ (NTf ₂) ₂].	S11
Fig. S4 Plots of UV-vis and fluorescence maxima (λ_{MAX}) recorded in different solvents at 298 K for: (a) and (b) [<i>p</i> -C ₈ Br ₂]; (c) and (d) [<i>p</i> -C ₁₂ Br ₂]; (e) and (f) [<i>p</i> -C ₈ (NTf ₂) ₂]; (g) and (h) [<i>p</i> -C ₁₂ (NTf ₂) ₂]; (i) <i>m</i> -C ₁₂ (NTf ₂) ₂ .	S12
Fig. S5 Plots of apparent absorption coefficient as a function of salt concentration corresponding to: (a) [<i>p</i> -C ₈ Br ₂] in ACN; (b) [<i>p</i> -C ₈ Br ₂] in THF; (c) [<i>p</i> -C ₁₂ Br ₂] in 1-PrOH; (d) [<i>p</i> -C ₁₂ Br ₂] in 2-PrOH; (e) [<i>p</i> -C ₁₂ Br ₂] in CHCl ₃ ; (f) [<i>p</i> -C ₈ (NTf ₂) ₂] in 2-PrOH; (g) [<i>p</i> -C ₈ (NTf ₂) ₂] in CHCl ₃ ; (h) [<i>p</i> -C ₈ (NTf ₂) ₂] in 1,4-Diox; (i) [<i>p</i> -C ₁₂ (NTf ₂) ₂] in ACN; (j) [<i>p</i> -C ₁₂ (NTf ₂) ₂] in THF; (k) [<i>m</i> -C ₁₂ (NTf ₂) ₂] in 1-PrOH; (l) [<i>m</i> -C ₁₂ (NTf ₂) ₂] in CHCl ₃ .	S14
Fig. S6 Plots of fluorescence intensity as a function of salt concentration corresponding to: (a) [<i>p</i> -C ₈ Br ₂] in ACN; (b) [<i>p</i> -C ₈ Br ₂] in THF; (c) [<i>p</i> -C ₁₂ Br ₂] in 1-PrOH; (d) [<i>p</i> -C ₁₂ Br ₂] in 2-PrOH; (e) [<i>p</i> -C ₁₂ Br ₂] in CHCl ₃ ; (f) [<i>p</i> -C ₈ (NTf ₂) ₂] in 2-PrOH; (g) [<i>p</i> -C ₈ (NTf ₂) ₂] in CHCl ₃ ; (h) [<i>p</i> -C ₈ (NTf ₂) ₂] in 1,4-Diox; (i) [<i>p</i> -C ₁₂ (NTf ₂) ₂] in ACN; (j) [<i>p</i> -C ₁₂ (NTf ₂) ₂] in THF.	S16
Fig. S7 Stern-Volmer plots corresponding to: (a) [<i>p</i> -C ₈ Br ₂] in ACN; (b) [<i>p</i> -C ₈ Br ₂] in THF; (c) [<i>p</i> -C ₁₂ Br ₂] in 1-PrOH; (d) [<i>p</i> -C ₁₂ Br ₂] in 2-PrOH; (e) [<i>p</i> -C ₁₂ Br ₂] in CHCl ₃ ; (f) [<i>p</i> -C ₈ (NTf ₂) ₂] in 2-PrOH; (g) [<i>p</i> -C ₈ (NTf ₂) ₂] in CHCl ₃ ; (h) [<i>p</i> -C ₈ (NTf ₂) ₂] in 1,4-Diox; (i) [<i>p</i> -C ₁₂ (NTf ₂) ₂] in ACN; (j) [<i>p</i> -C ₁₂ (NTf ₂) ₂] in THF.	S18
Fig. S8 Plots of RLS intensity as a function of salt concentration corresponding to: (a) [<i>p</i> -C ₈ Br ₂] in ACN; (b) [<i>p</i> -C ₈ Br ₂] in THF; (c) [<i>p</i> -C ₁₂ Br ₂] in 1-PrOH; (d) [<i>p</i> -C ₁₂ Br ₂] in 2-PrOH; (e) [<i>p</i> -C ₁₂ Br ₂] in CHCl ₃ ; (f) [<i>p</i> -C ₈ (NTf ₂) ₂] in 2-PrOH; (g) [<i>p</i> -C ₈ (NTf ₂) ₂] in CHCl ₃ ; (h) [<i>p</i> -C ₈ (NTf ₂) ₂] in 1,4-Diox; (i) [<i>p</i> -C ₁₂ (NTf ₂) ₂] in ACN; (j) [<i>p</i> -C ₁₂ (NTf ₂) ₂] in THF.	S19
Fig. S9 SEM images collected from casting of $1 \cdot 10^{-4}$ M solution. (a) [<i>p</i> -C ₈ Br ₂]/ACN; (b), (c) [<i>p</i> -C ₈ Br ₂]/THF; (d) [<i>p</i> -C ₁₂ Br ₂]/1-PrOH; (e), (f) [<i>p</i> -C ₁₂ Br ₂]/CHCl ₃ ; (g) [<i>p</i> -C ₈ (NTf ₂) ₂]/2-PrOH; (h) [<i>p</i> -C ₈ (NTf ₂) ₂]/CHCl ₃ ; (i), (j) [<i>p</i> -C ₈ (NTf ₂) ₂]/1,4-Diox; (k) [<i>p</i> -C ₁₂ (NTf ₂) ₂]/ACN; (l) [<i>p</i> -C ₁₂ (NTf ₂) ₂]/1-PrOH; (m) [<i>m</i> -C ₁₂ (NTf ₂) ₂]/1-PrOH; (n), (o) [<i>m</i> -C ₁₂ (NTf ₂) ₂]/CHCl ₃ .	S21
Fig. S10 Fluorescence spectra in solution (red line) and in solid state (blue line) corresponding to: (a) [<i>p</i> -C ₈ Br ₂] in ACN; (b) [<i>p</i> -C ₈ Br ₂] in THF; (c) [<i>p</i> -C ₁₂ Br ₂] in 1-PrOH; (d) [<i>p</i> -C ₁₂ Br ₂] in 2-PrOH; (e) [<i>p</i> -C ₁₂ Br ₂] in CHCl ₃ ; (f) [<i>p</i> -C ₈ (NTf ₂) ₂] in 2-PrOH; (g) [<i>p</i> -C ₈ (NTf ₂) ₂] in CHCl ₃ ; (h) [<i>p</i> -C ₈ (NTf ₂) ₂] in 1,4-Diox; (i) [<i>p</i> -C ₁₂ (NTf ₂) ₂] in ACN; (j) [<i>p</i> -C ₁₂ (NTf ₂) ₂] in 1-PrOH; (k) [<i>p</i> -C ₁₂ (NTf ₂) ₂] in THF.	S23
Fig. S11 (a) Solution and (b) deconvoluted solid state spectra for [<i>p</i> -C ₁₂ (NTf ₂) ₂] in 1-PrOH.	S25
Table S1 RLS Intensity at 378 nm as function of salt and solvent nature ([salt] = $1 \cdot 10^{-4}$ M)	S25
Table S2 Estimated size of solvent molecules on the base of DFT geometries and AMBER atomic radii	S25
Table S3 λ_{MAX} and $\Delta\lambda$ values detected for fluorescence spectra recorded in solution and solid state at $1 \cdot 10^{-4}$ M.	S26

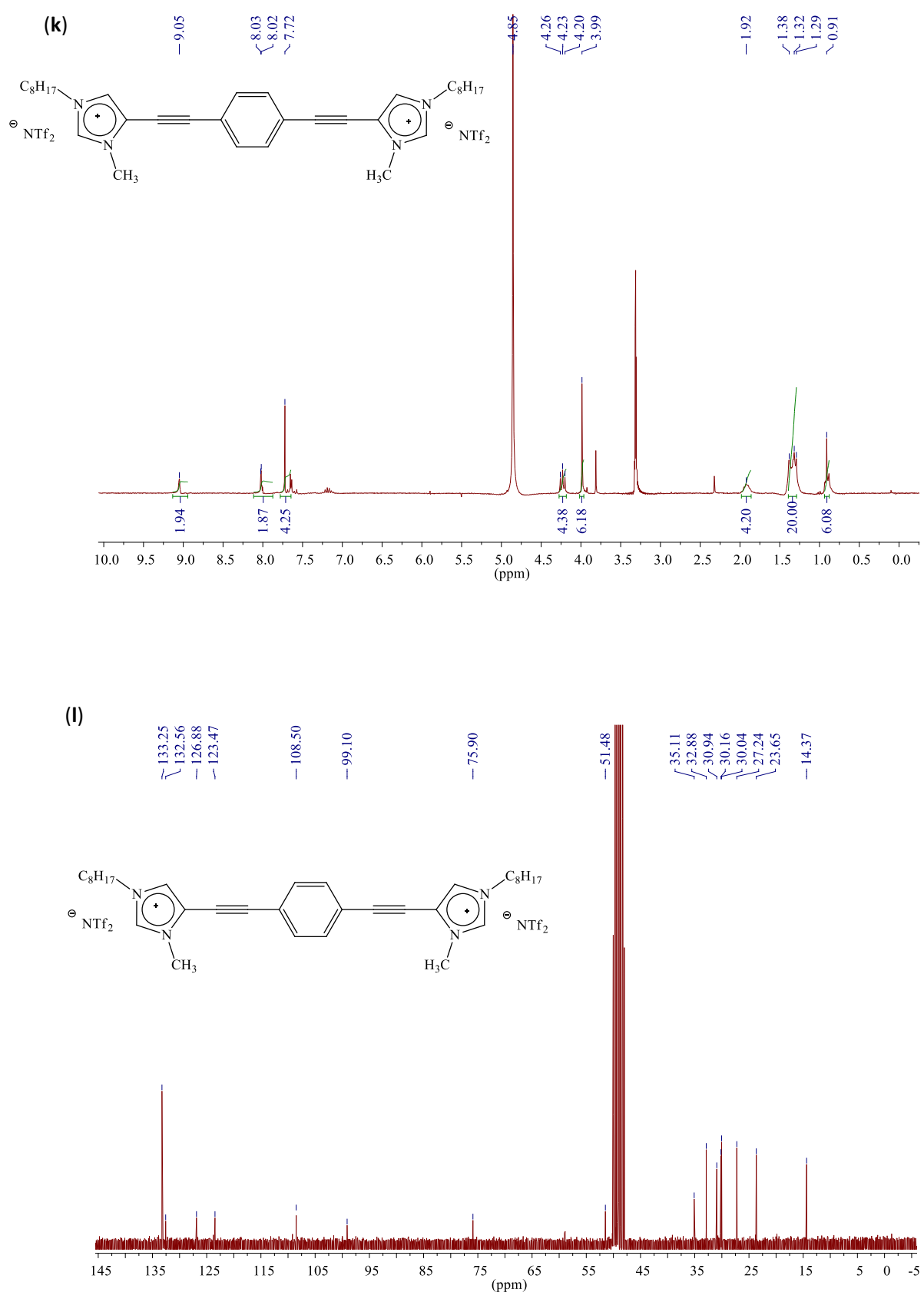




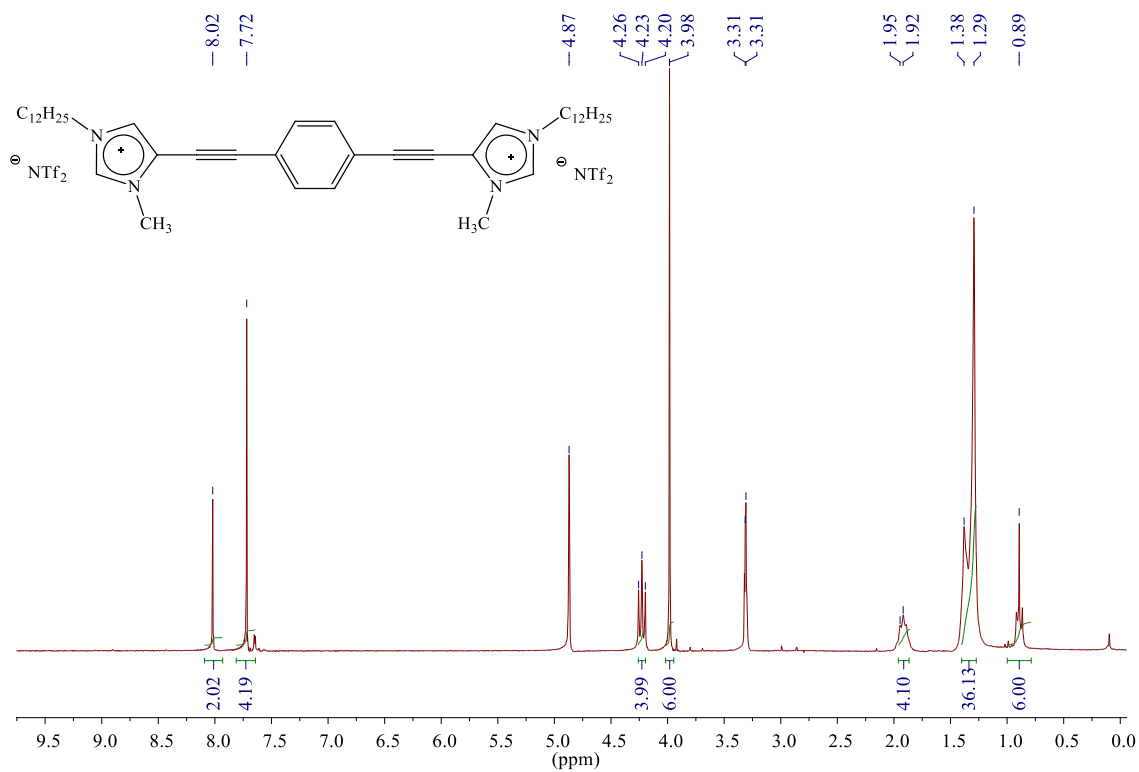




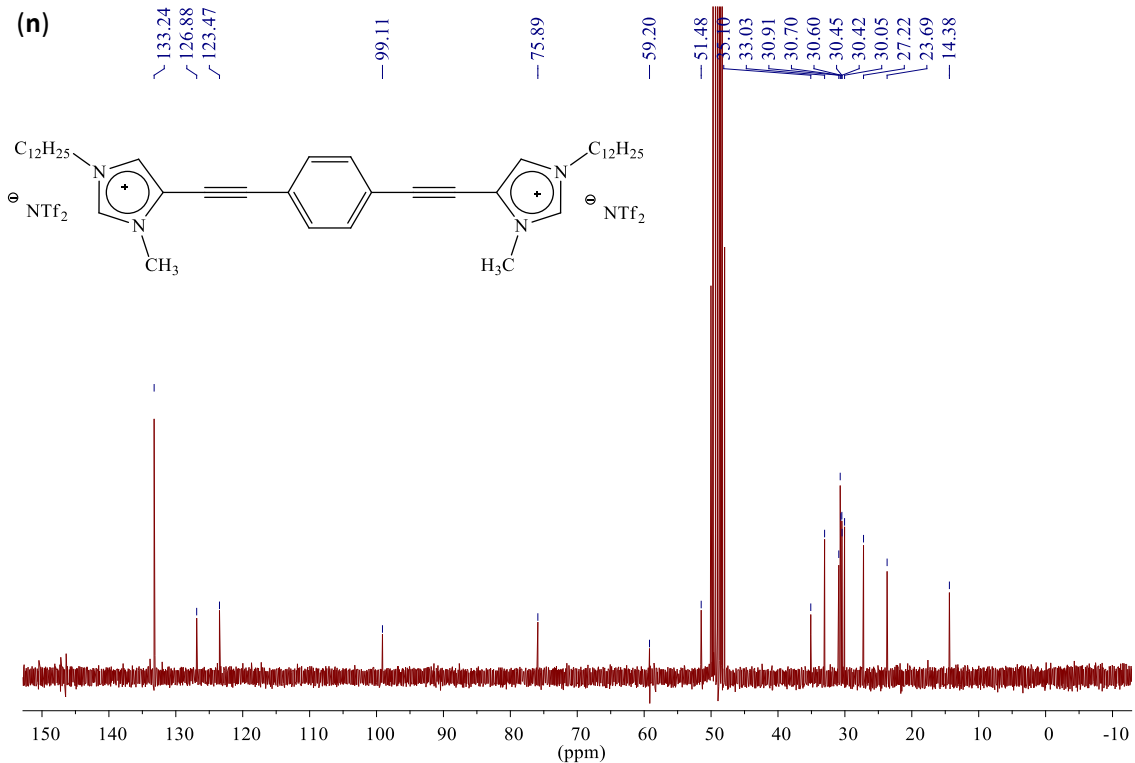




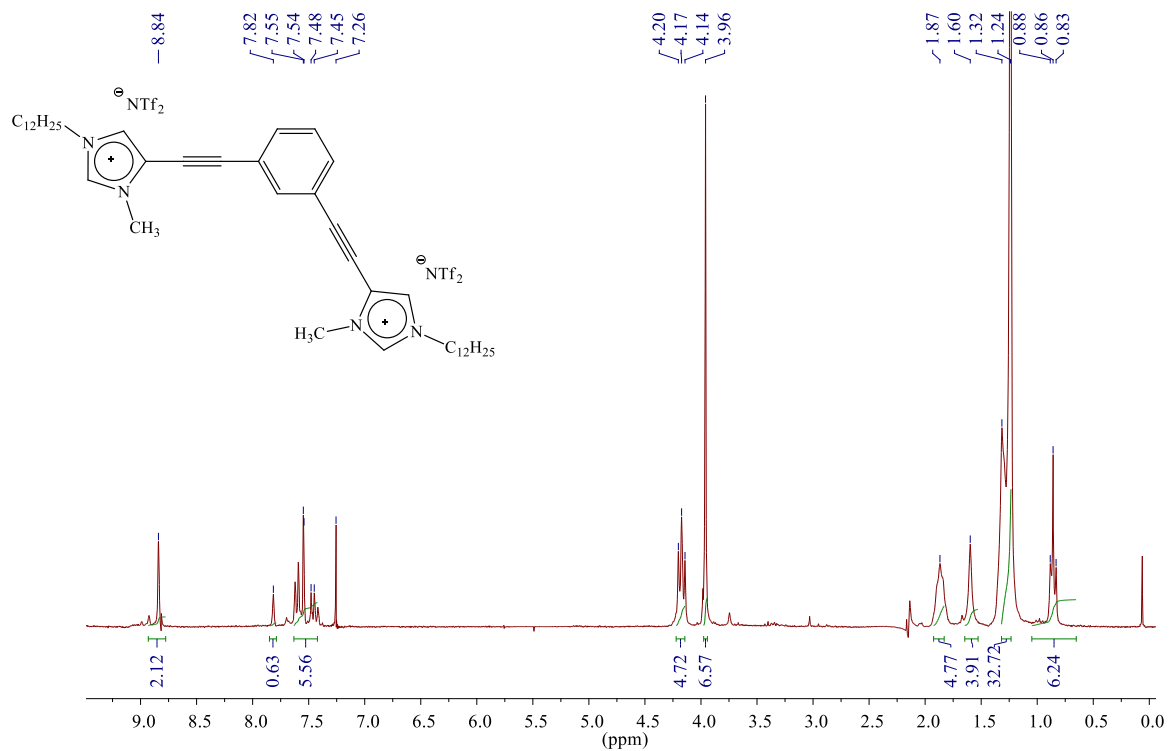
(m)



(n)



(o)



(p)

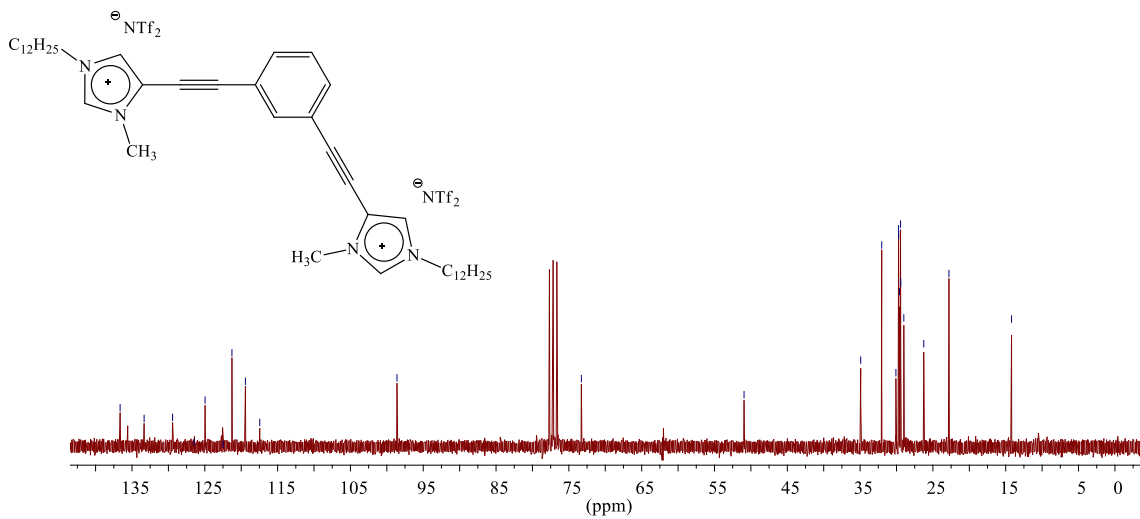
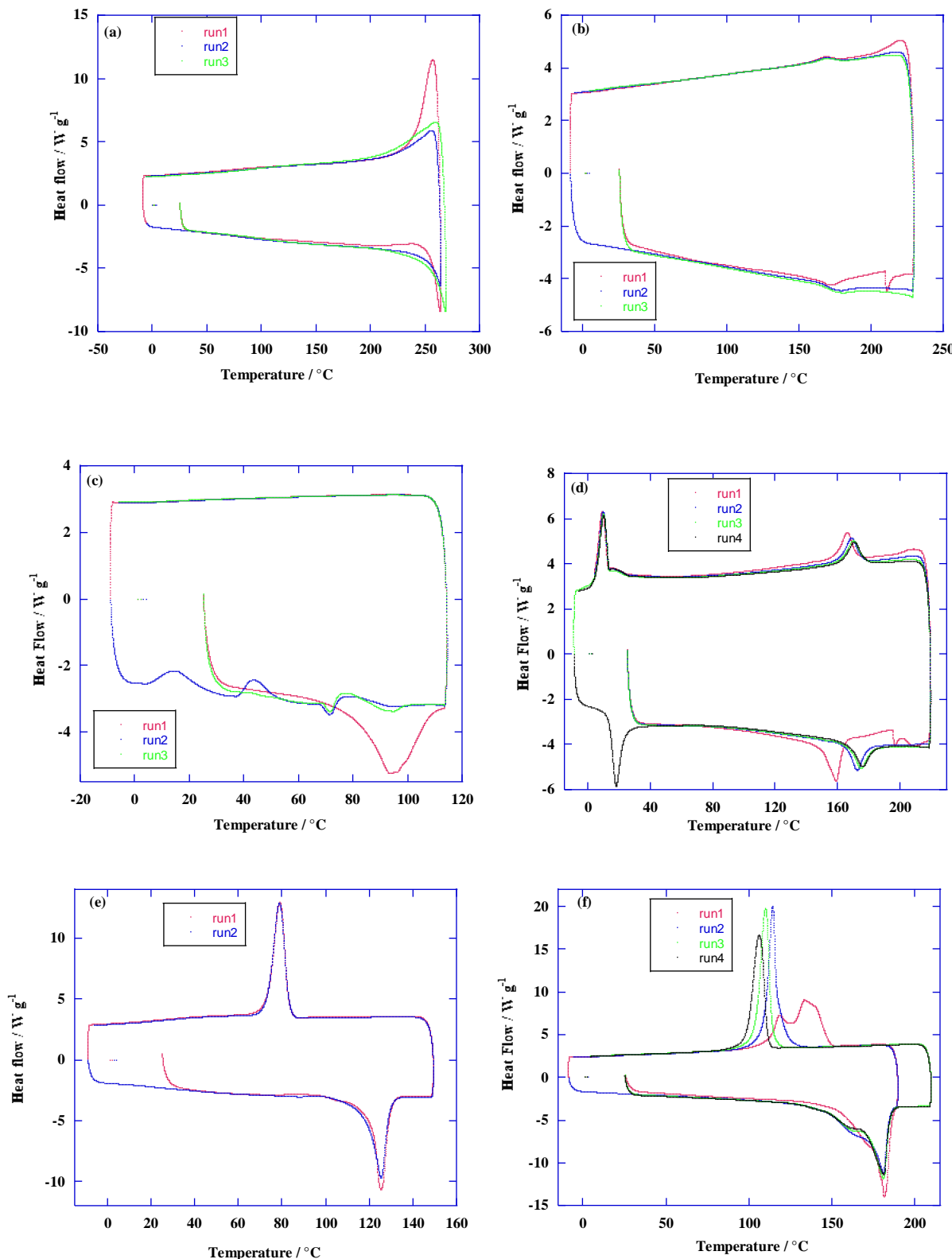


Fig. S1 ^1H NMR and ^{13}C NMR spectra corresponding to: (a), (b) **1**; (c), (d) **2**; (e), (f) [*p*-C₈Br₂]; (g), (h) [*p*-C₁₂Br₂]; (i), (j) [*m*-C₁₂Br₂]; (k), (l) [*p*-C₈(NTf₂)₂]; (m), (n) [*p*-C₁₂(NTf₂)₂] and (o), (p) [*m*-C₁₂(NTf₂)₂].



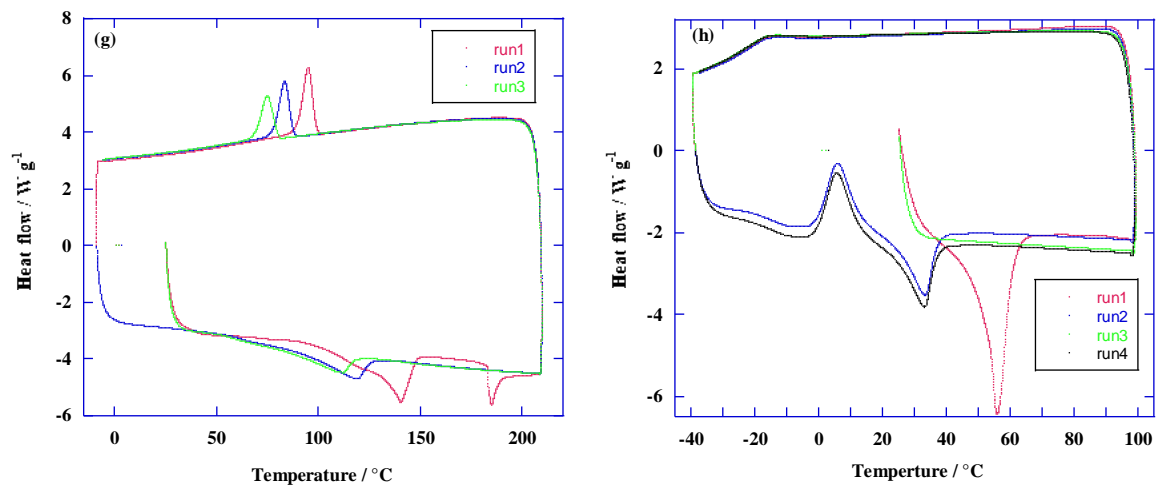
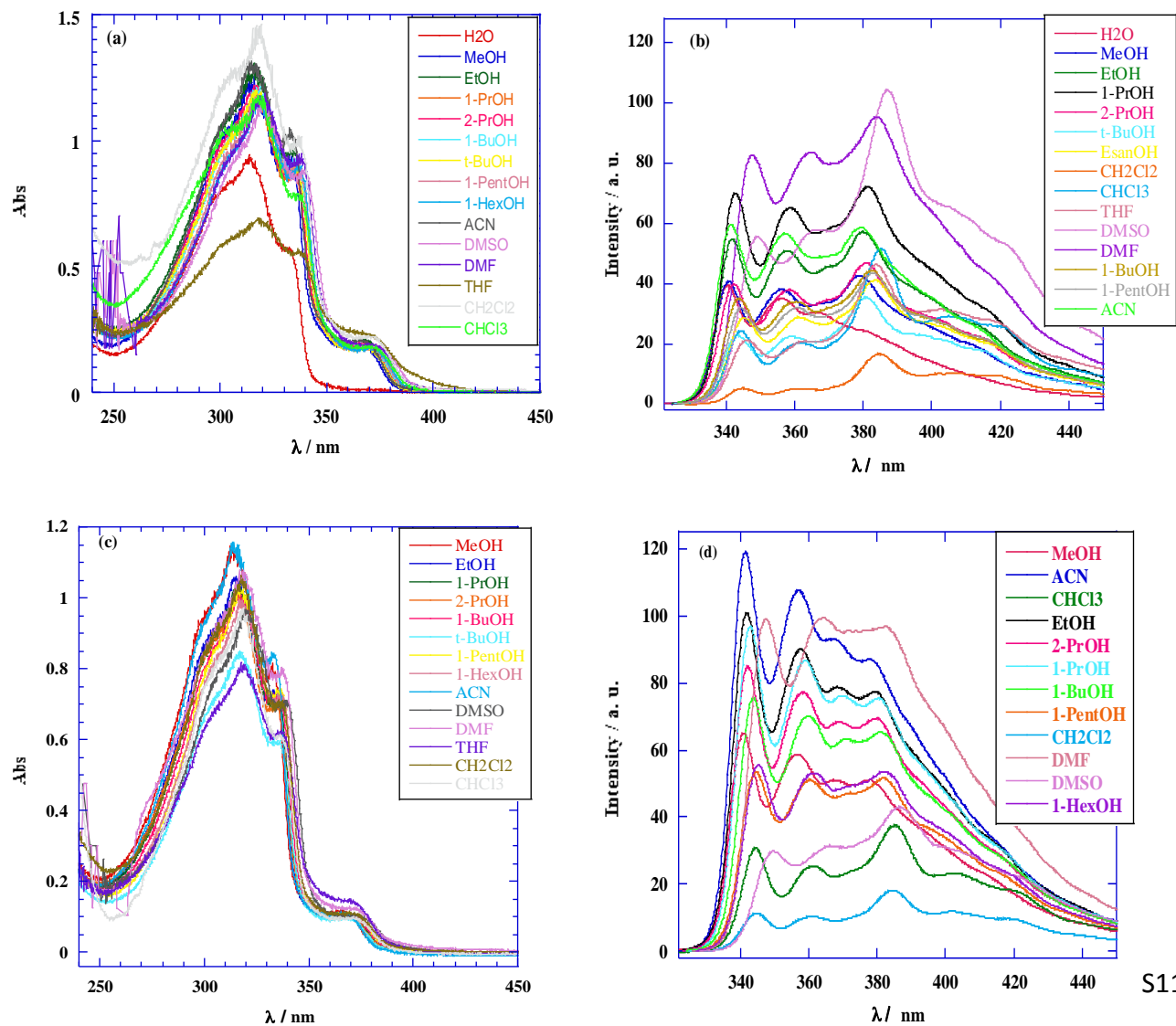


Fig. S2 DSC traces corresponding to: (a) **1**; (b) [*p*-C₈Br₂]; (c) [*p*-C₈(NTf₂)₂]; (d) [*p*-C₁₂Br₂]; (e) [*p*-C₁₂(NTf₂)₂]; (f) **2**; (g) [*m*-C₁₂Br₂]; (h) [*m*-C₁₂(NTf₂)₂] (exo up).



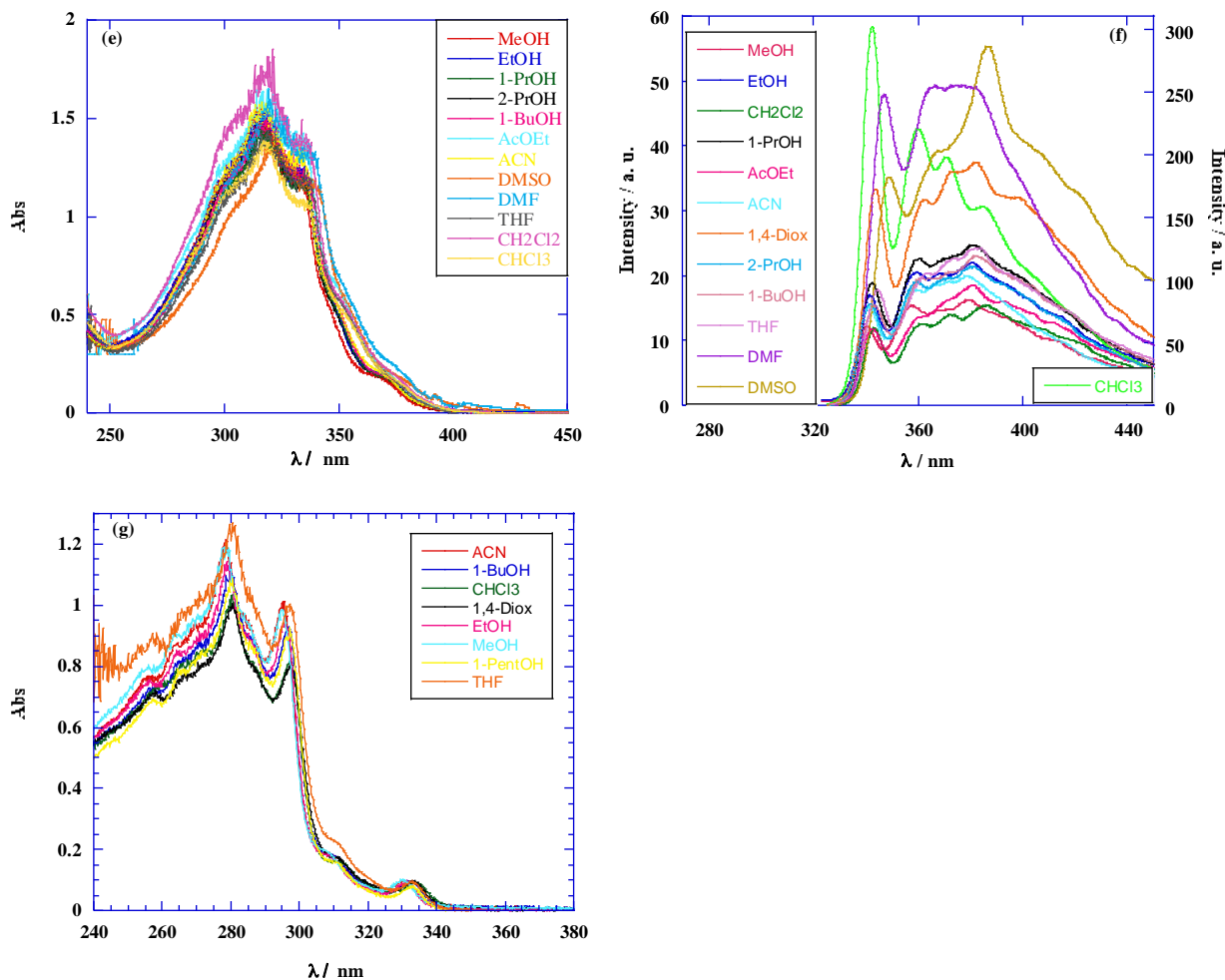
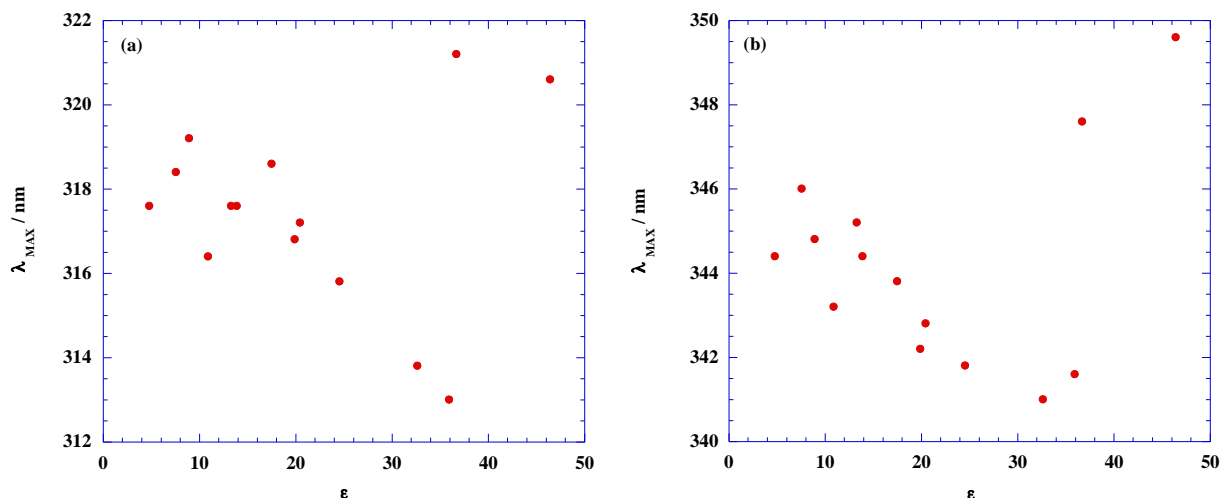
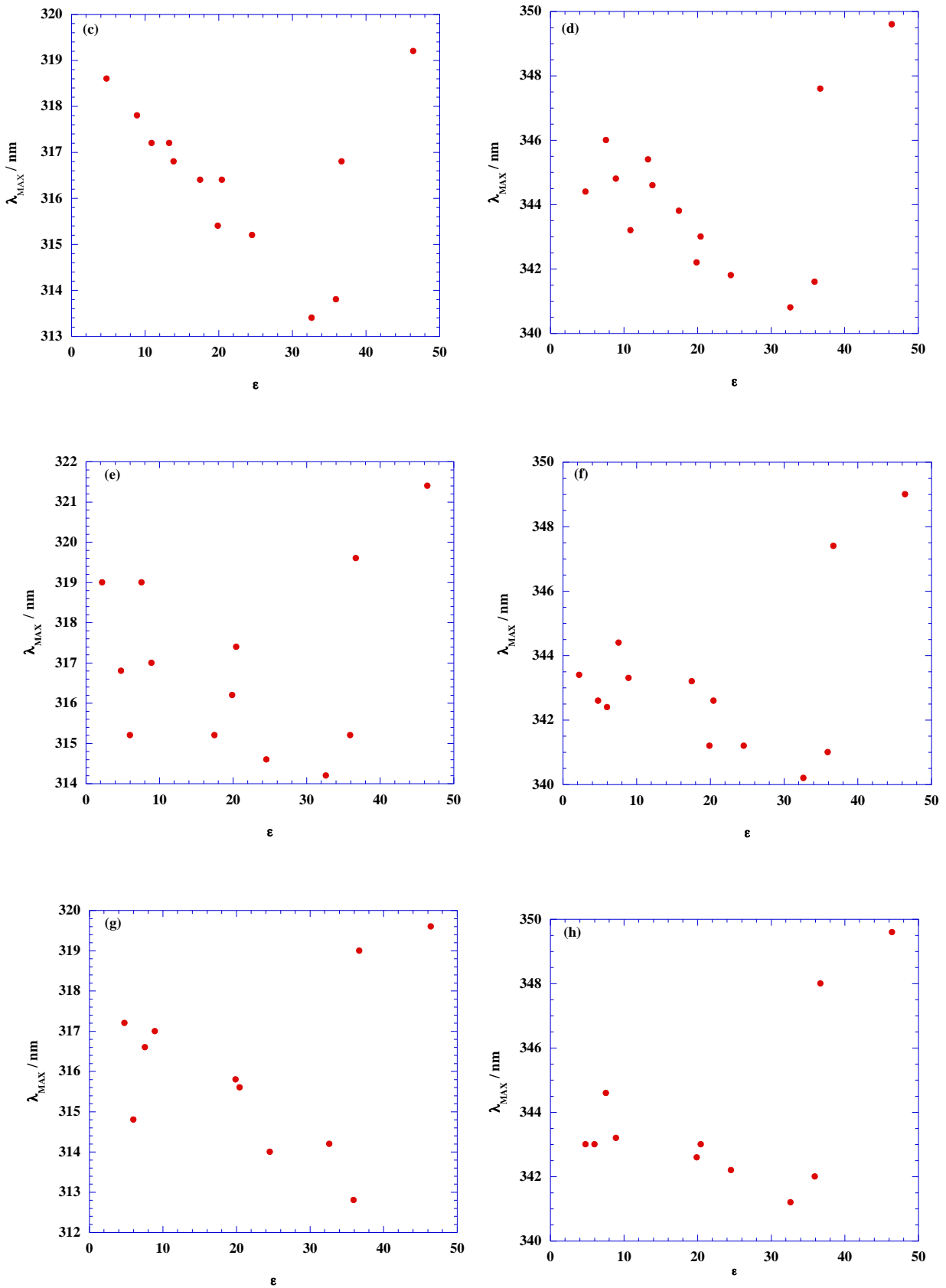


Fig. S3 UV-vis and fluorescence spectra recorded in different solvents at 298 K for: (a) and (b) [p-C₈Br₂]; (c) and (d) [p-C₁₂Br₂]; (e) and (f) [p-C₈(NTf₂)₂]; (g) [m-C₁₂(NTf₂)₂].





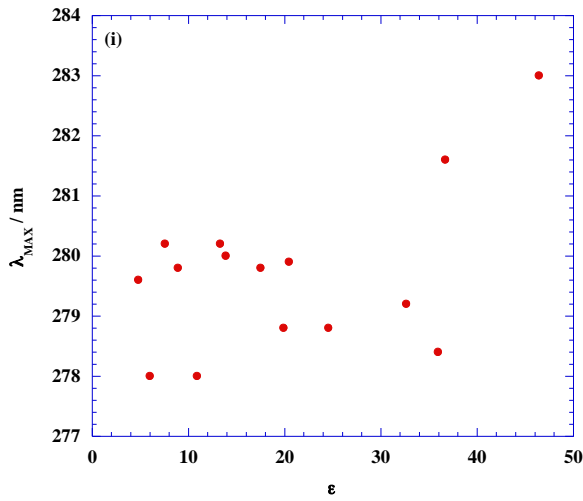
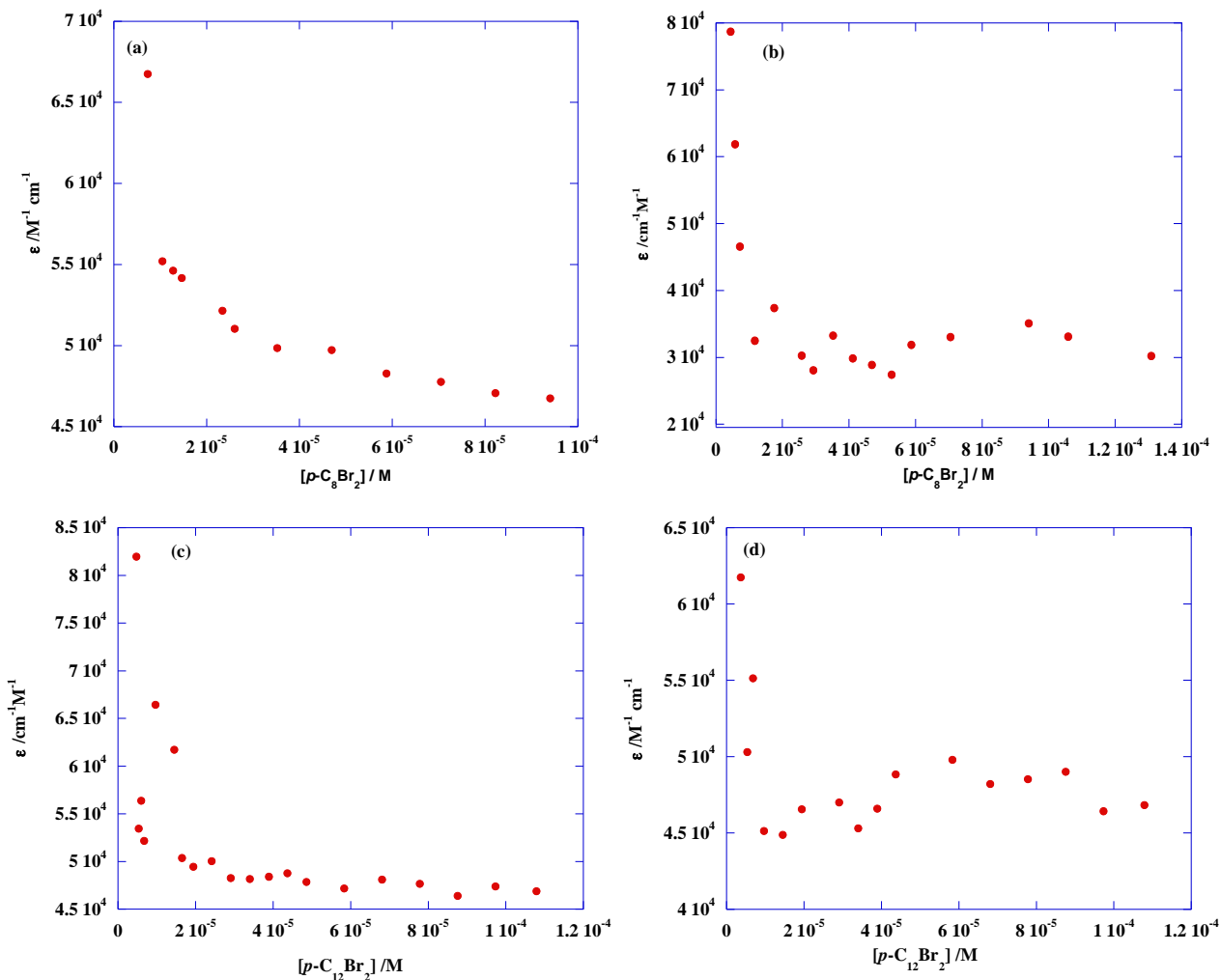
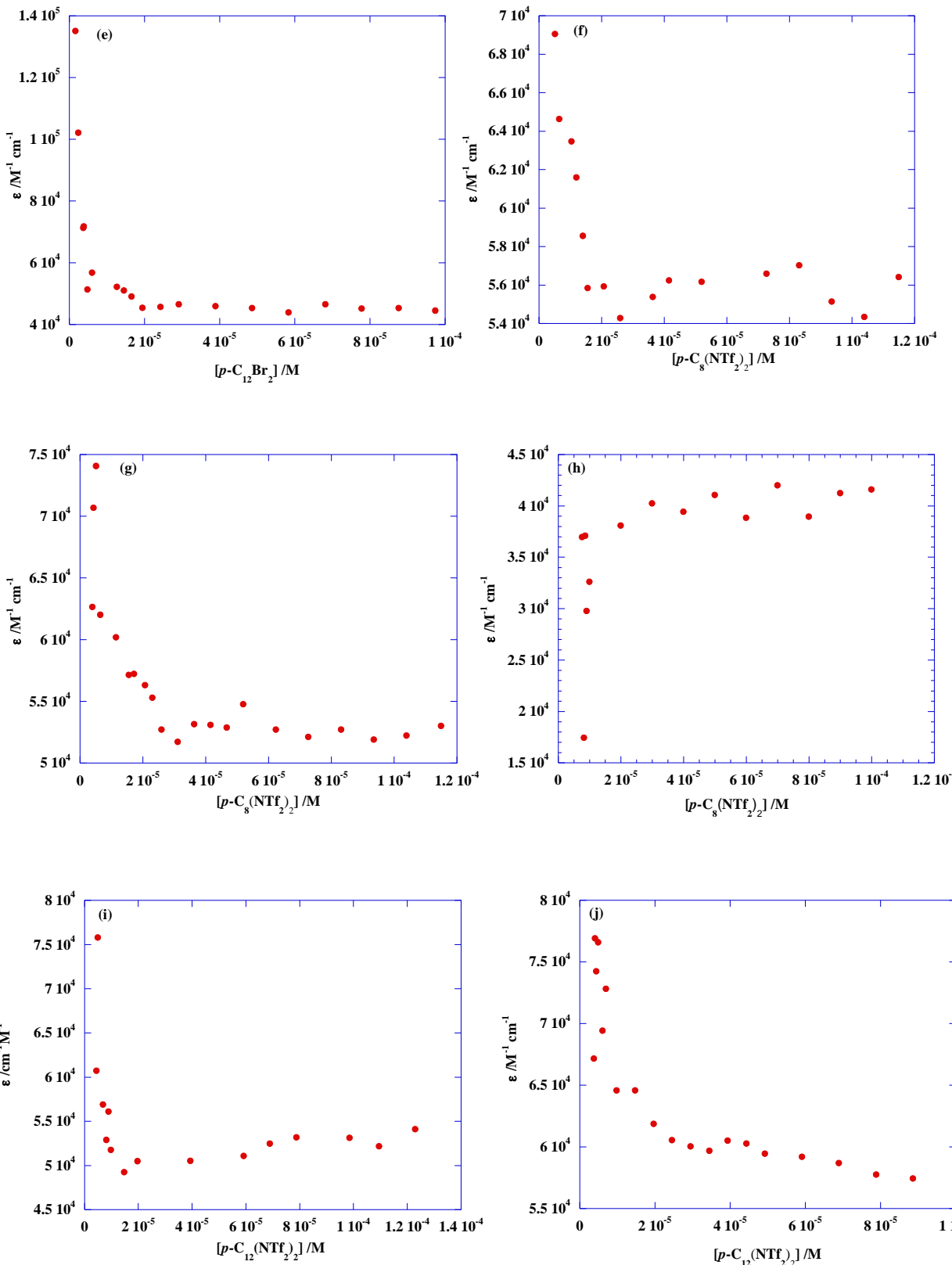


Fig. S4 Plots of UV-vis and fluorescence maxima (λ_{MAX}) recorded in different solvents at 298 K for: (a) and (b) [$p\text{-C}_8\text{Br}_2$]; (c) and (d) [$p\text{-C}_{12}\text{Br}_2$]; (e) and (f) [$p\text{-C}_8(\text{NTf}_2)_2$]; (g) and (h) [$p\text{-C}_{12}(\text{NTf}_2)_2$]; (i) $m\text{-C}_{12}(\text{NTf}_2)_2$.





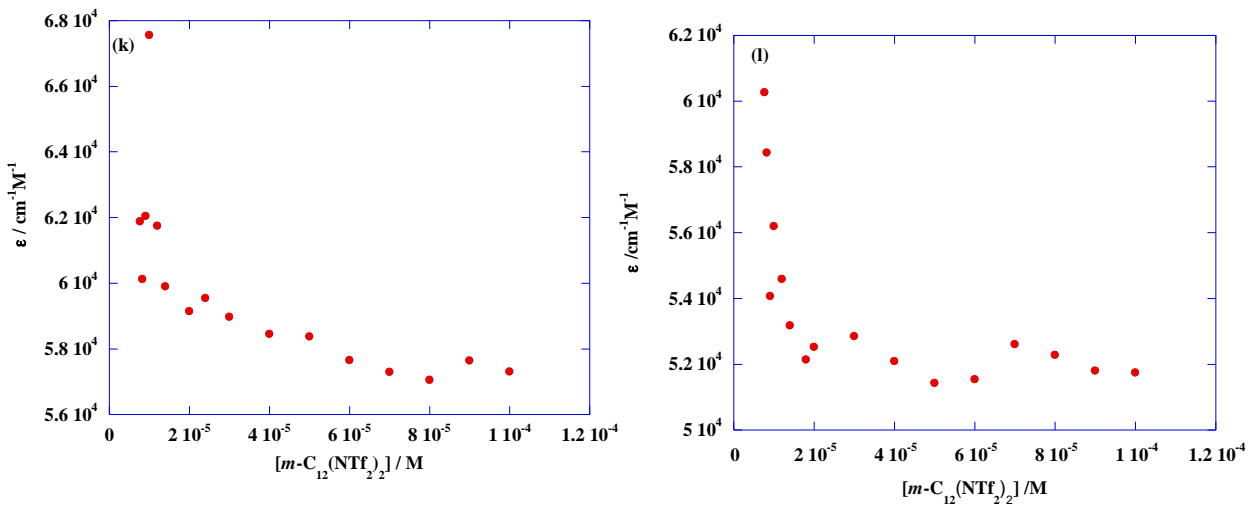
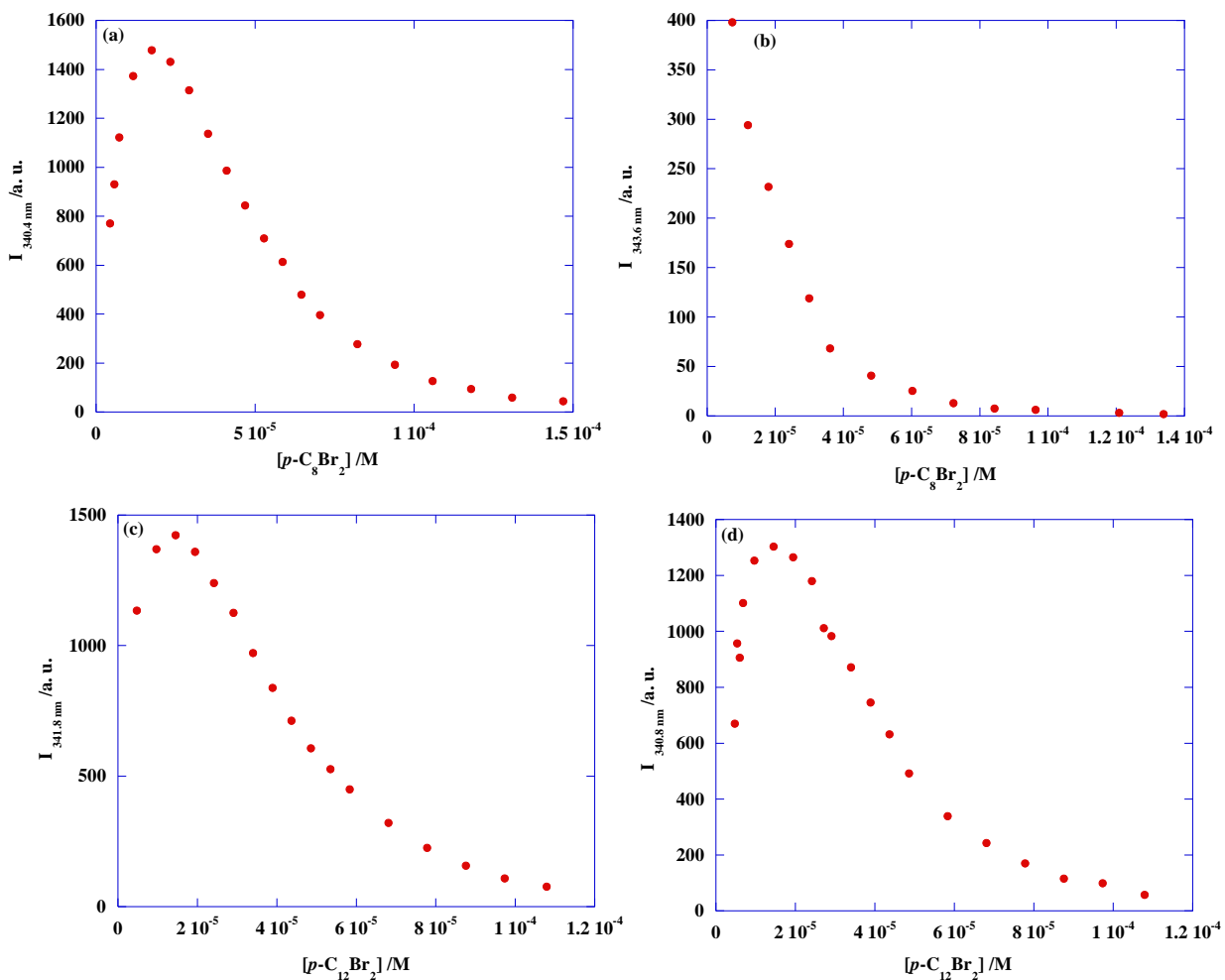


Fig. S5 Plots of apparent absorption coefficient as a function of salt concentration corresponding to: (a) $[p\text{-C}_8\text{Br}_2]$ in ACN; (b) $[p\text{-C}_8\text{Br}_2]$ in THF; (c) $[p\text{-C}_{12}\text{Br}_2]$ in 1-PrOH; (d) $[p\text{-C}_{12}\text{Br}_2]$ in 2-PrOH; (e) $[p\text{-C}_{12}\text{Br}_2]$ in CHCl_3 ; (f) $[p\text{-C}_8\text{(NTf}_2\text{)}_2]$ in 2-PrOH; (g) $[p\text{-C}_8\text{(NTf}_2\text{)}_2]$ in CHCl_3 ; (h) $[p\text{-C}_8\text{(NTf}_2\text{)}_2]$ in 1,4-Diox; (i) $[p\text{-C}_{12}\text{(NTf}_2\text{)}_2]$ in ACN; (j) $[p\text{-C}_{12}\text{(NTf}_2\text{)}_2]$ in THF; (k) $[m\text{-C}_{12}\text{(NTf}_2\text{)}_2]$ in 1-PrOH; (l) $[m\text{-C}_{12}\text{(NTf}_2\text{)}_2]$ in CHCl_3 .



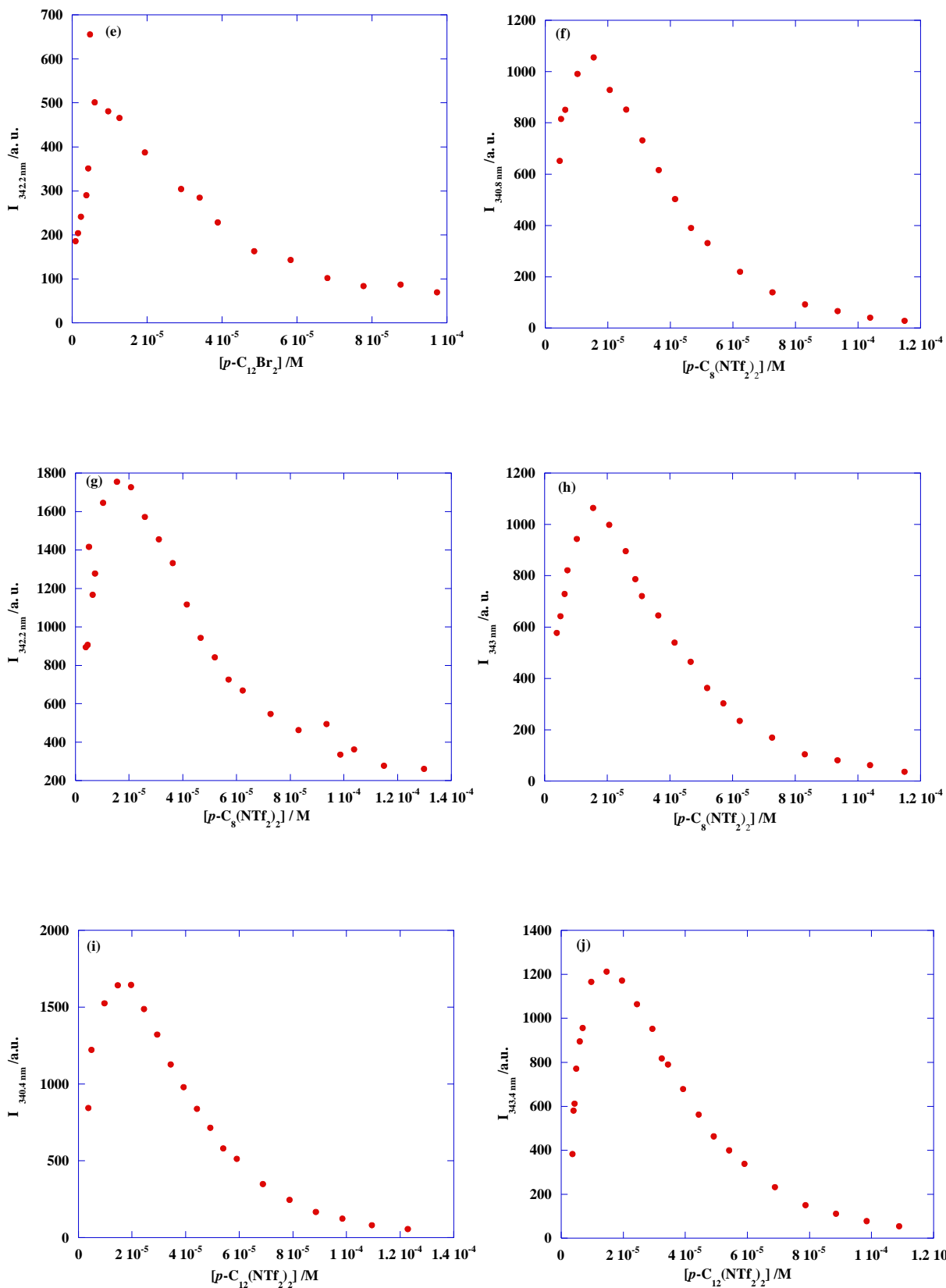
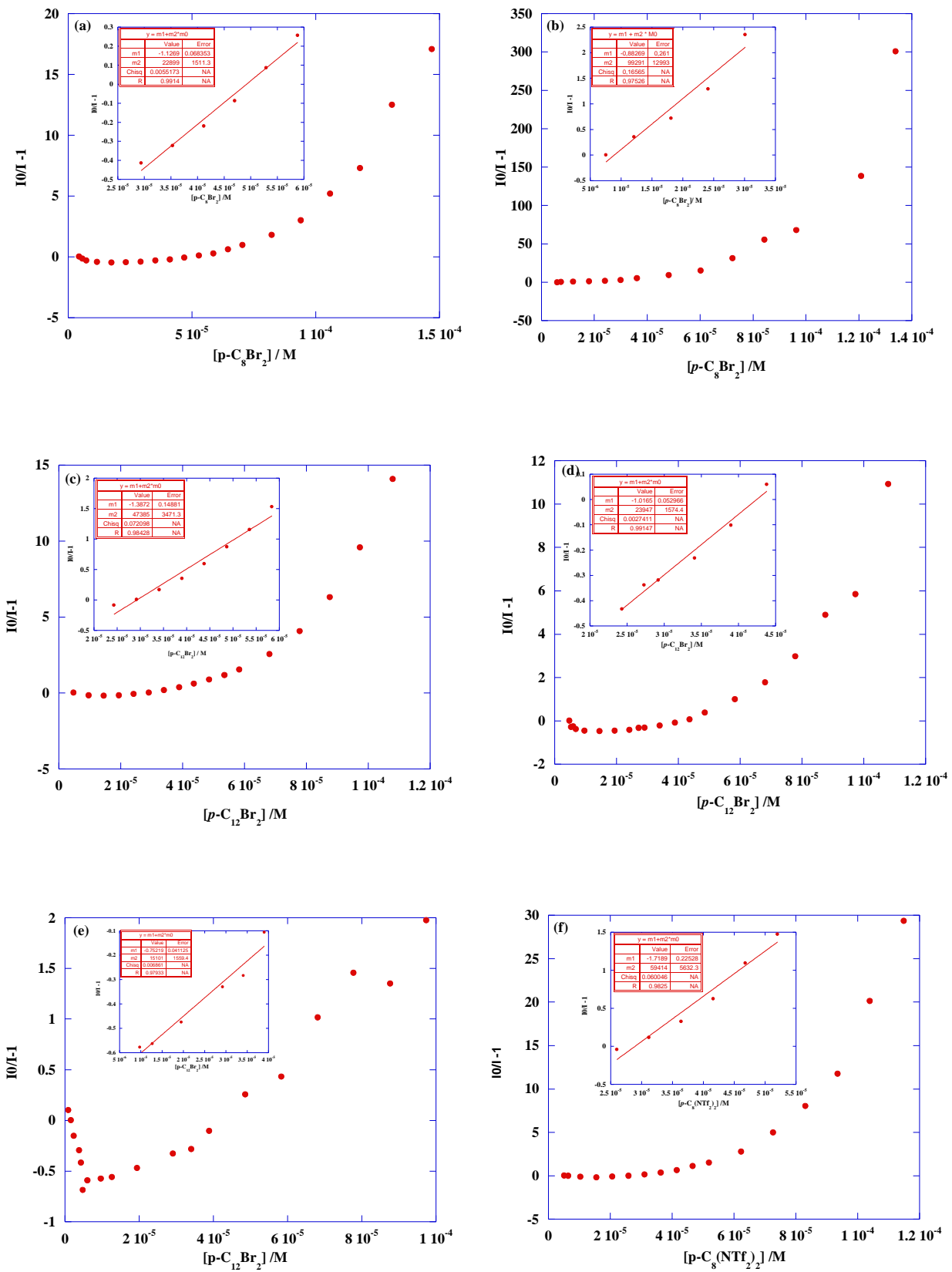


Fig. S6 Plots of fluorescence intensity as a function of salt concentration corresponding to: (a) $[p\text{-C}_8\text{Br}_2]$ in ACN; (b) $[p\text{-C}_8\text{Br}_2]$ in THF; (c) $[p\text{-C}_{12}\text{Br}_2]$ in 1-PrOH; (d) $[p\text{-C}_{12}\text{Br}_2]$ in 2-PrOH; (e) $[p\text{-C}_{12}\text{Br}_2]$ in CHCl₃; (f) $[p\text{-C}_8(\text{NTf}_2)_2]$ in 2-PrOH; (g) $[p\text{-C}_8(\text{NTf}_2)_2]$ in CHCl₃; (h) $[p\text{-C}_8(\text{NTf}_2)_2]$ in 1,4-Diox; (i) $[p\text{-C}_{12}(\text{NTf}_2)_2]$ in ACN; (j) $[p\text{-C}_{12}(\text{NTf}_2)_2]$ in THF.



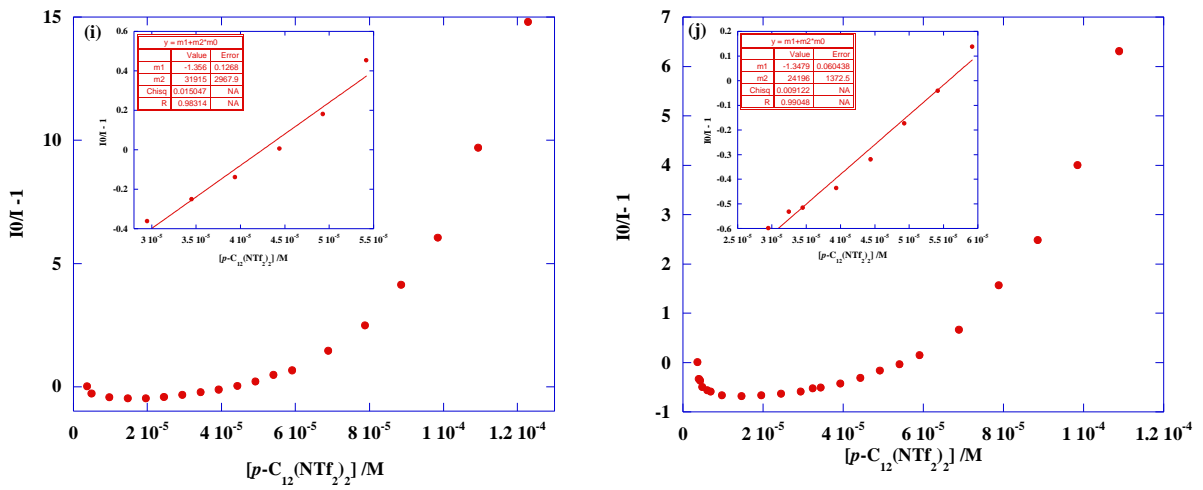
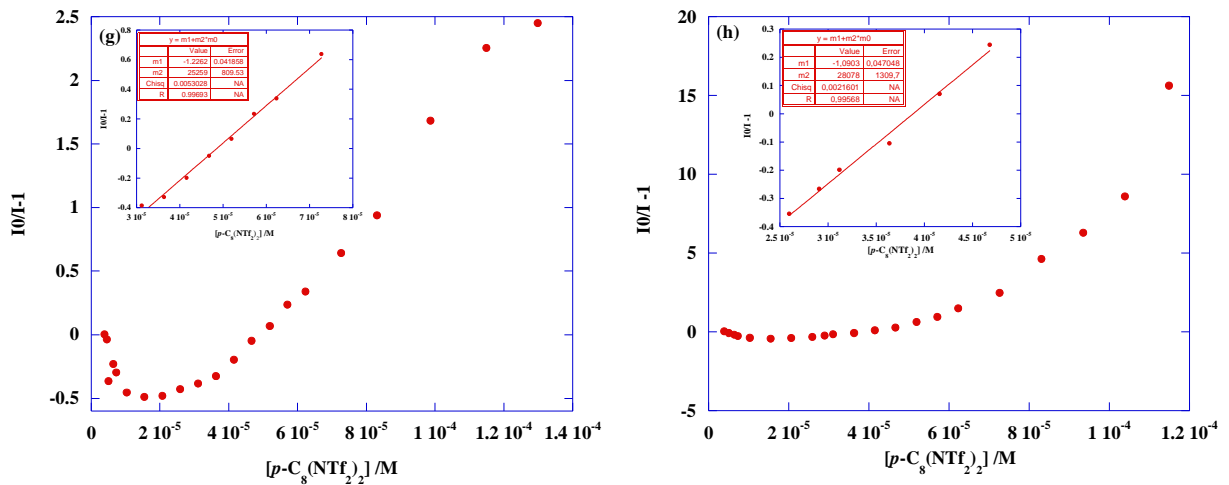
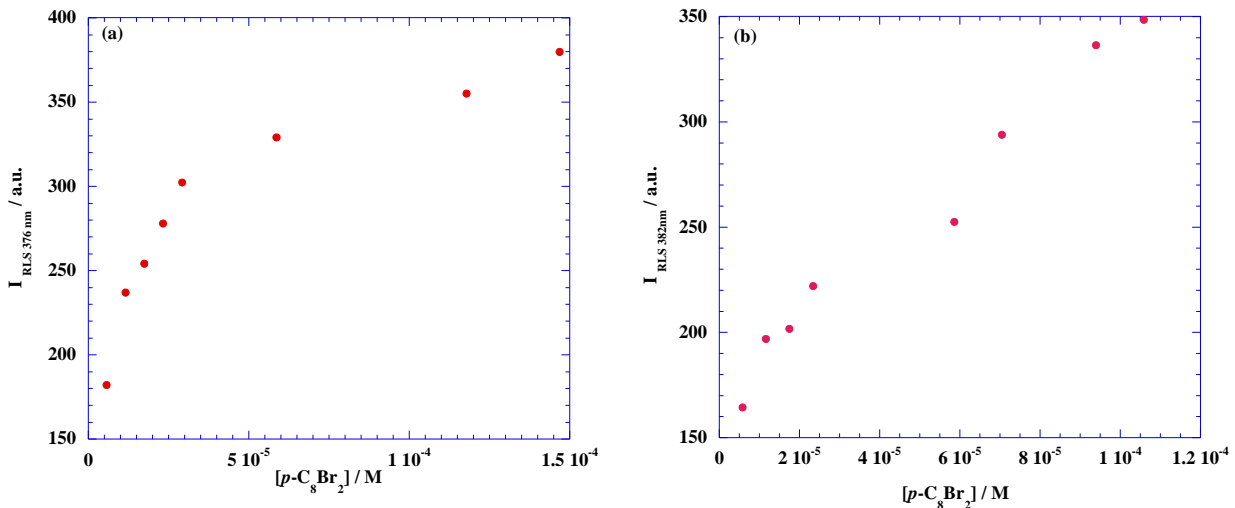
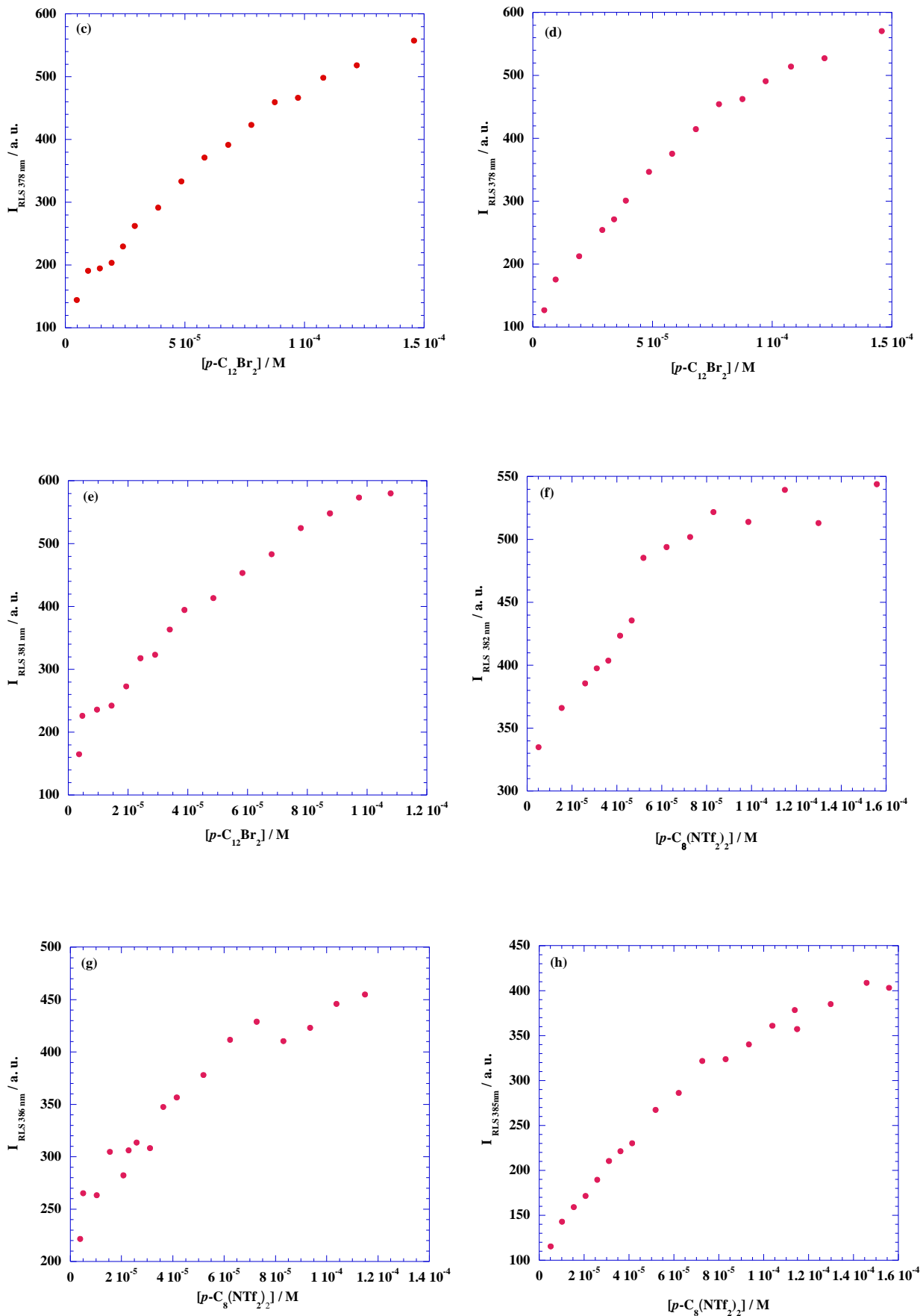


Fig. S7 Stern-Volmer plots corresponding to: (a) $[p\text{-C}_8\text{Br}_2]$ in ACN; (b) $[p\text{-C}_8\text{Br}_2]$ in THF; (c) $[p\text{-C}_{12}\text{Br}_2]$ in 1-PrOH; (d) $[p\text{-C}_{12}\text{Br}_2]$ in 2-PrOH; (e) $[p\text{-C}_{12}\text{Br}_2]$ in CHCl_3 ; (f) $[p\text{-C}_8(\text{NTf}_2)_2]$ in 2-PrOH; (g) $[p\text{-C}_8(\text{NTf}_2)_2]$ in CHCl_3 ; (h) $[p\text{-C}_8(\text{NTf}_2)_2]$ in 1,4-Diox; (i) $[p\text{-C}_{12}(\text{NTf}_2)_2]$ in ACN; (j) $[p\text{-C}_{12}(\text{NTf}_2)_2]$ in THF.





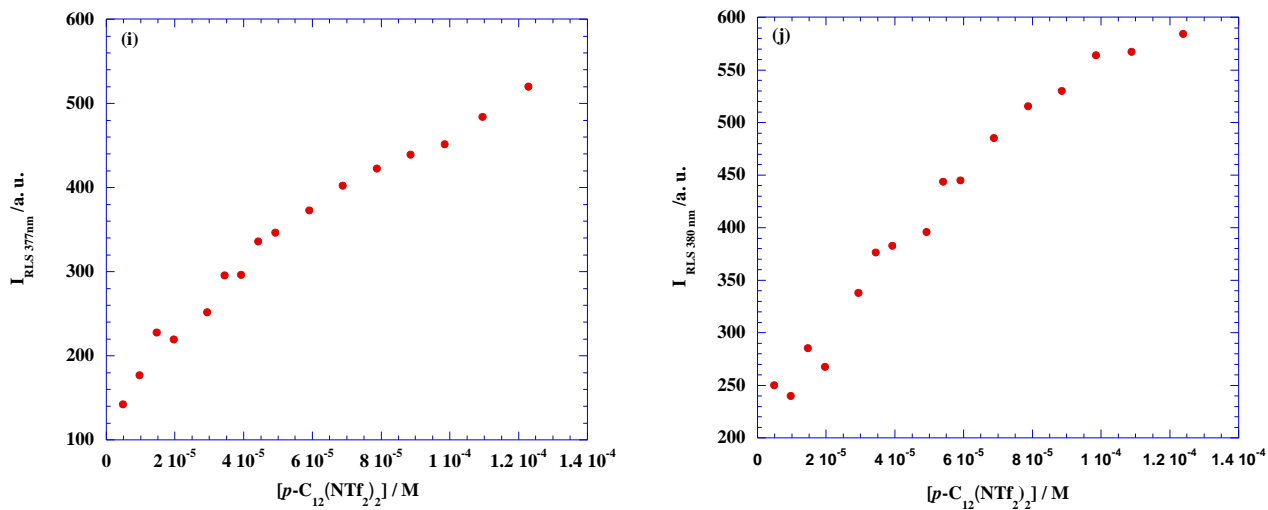
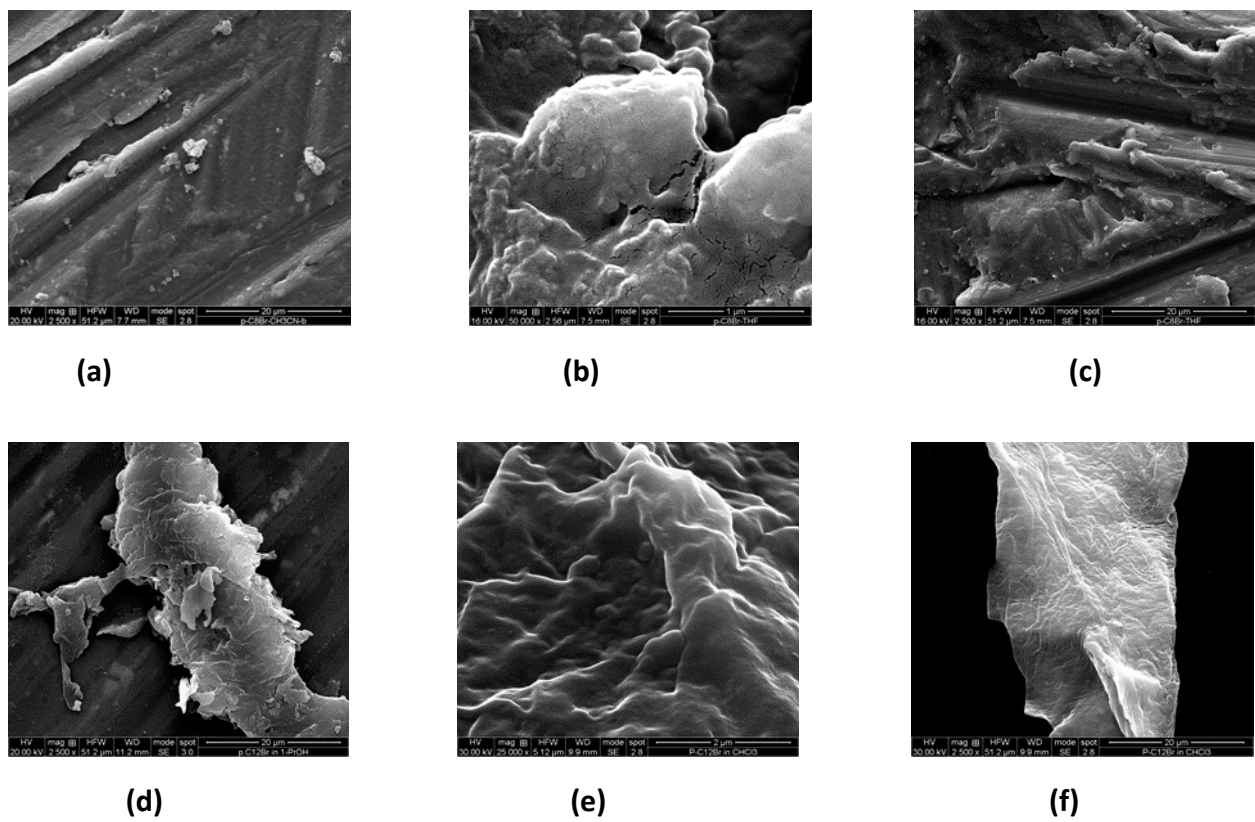
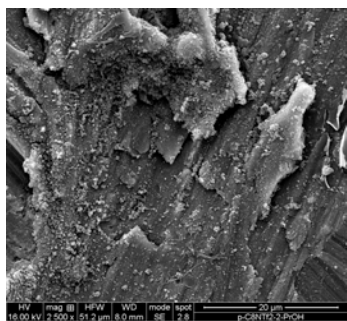
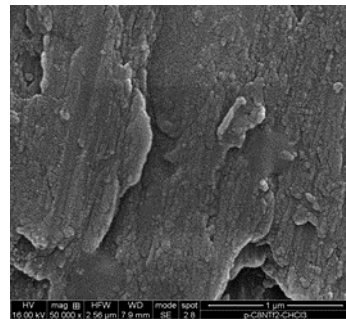


Fig. S8 Plots of RLS intensity as a function of salt concentration corresponding to: (a) $[p\text{-C}_8\text{Br}_2]$ in ACN; (b) $[p\text{-C}_8\text{Br}_2]$ in THF; (c) $[p\text{-C}_{12}\text{Br}_2]$ in 1-PrOH; (d) $[p\text{-C}_{12}\text{Br}_2]$ in 2-PrOH; (e) $[p\text{-C}_{12}\text{Br}_2]$ in CHCl_3 ; (f) $[p\text{-C}_8(\text{NTf}_2)_2]$ in 2-PrOH; (g) $[p\text{-C}_8(\text{NTf}_2)_2]$ in CHCl_3 ; (h) $[p\text{-C}_8(\text{NTf}_2)_2]$ in 1,4-Diox; (i) $[p\text{-C}_{12}(\text{NTf}_2)_2]$ in ACN; (j) $[p\text{-C}_{12}(\text{NTf}_2)_2]$ in THF.

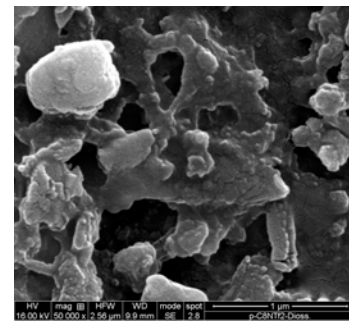




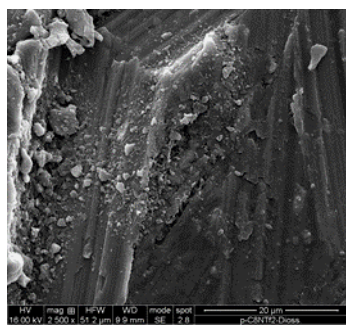
(g)



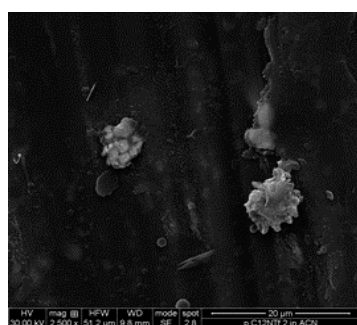
(h)



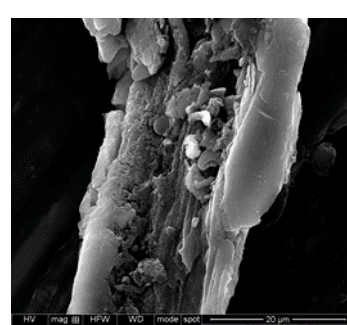
(i)



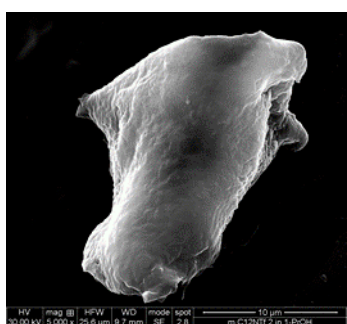
(j)



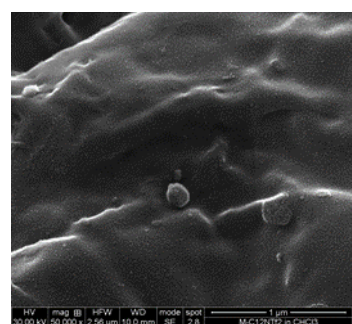
(k)



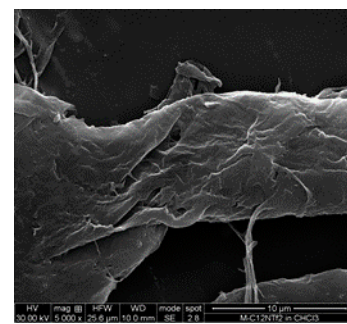
(l)



(m)

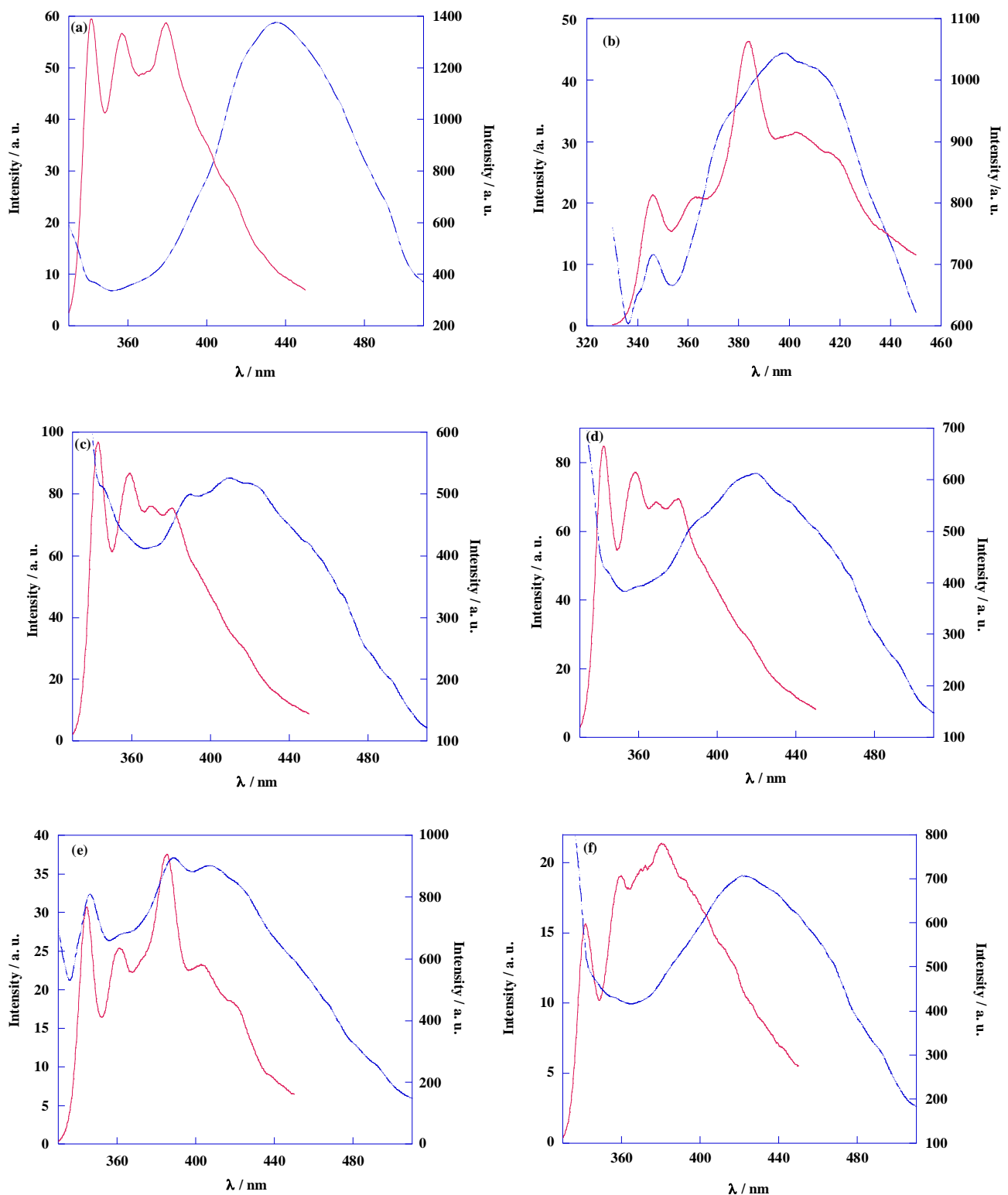


(n)



(o)

Fig. S9 SEM images collected from casting of 0.0001 M solution. (a) [p-C₈Br₂]/ACN; (b), (c) [p-C₈Br₂]/THF; (d) [p-C₁₂Br₂]/1-PrOH; (e), (f) [p-C₁₂Br₂]/CHCl₃; (g) [p-C₈(NTf₂)₂]/2-PrOH; (h) [p-C₈(NTf₂)₂]/CHCl₃; (i), (j) [p-C₈(NTf₂)₂]/1,4-Diox; (k) [p-C₁₂(NTf₂)₂]/ACN; (l) [p-C₁₂(NTf₂)₂]/1-PrOH; (m) [m-C₁₂(NTf₂)₂]/1-PrOH; (n), (o) [m-C₁₂(NTf₂)₂]/CHCl₃.



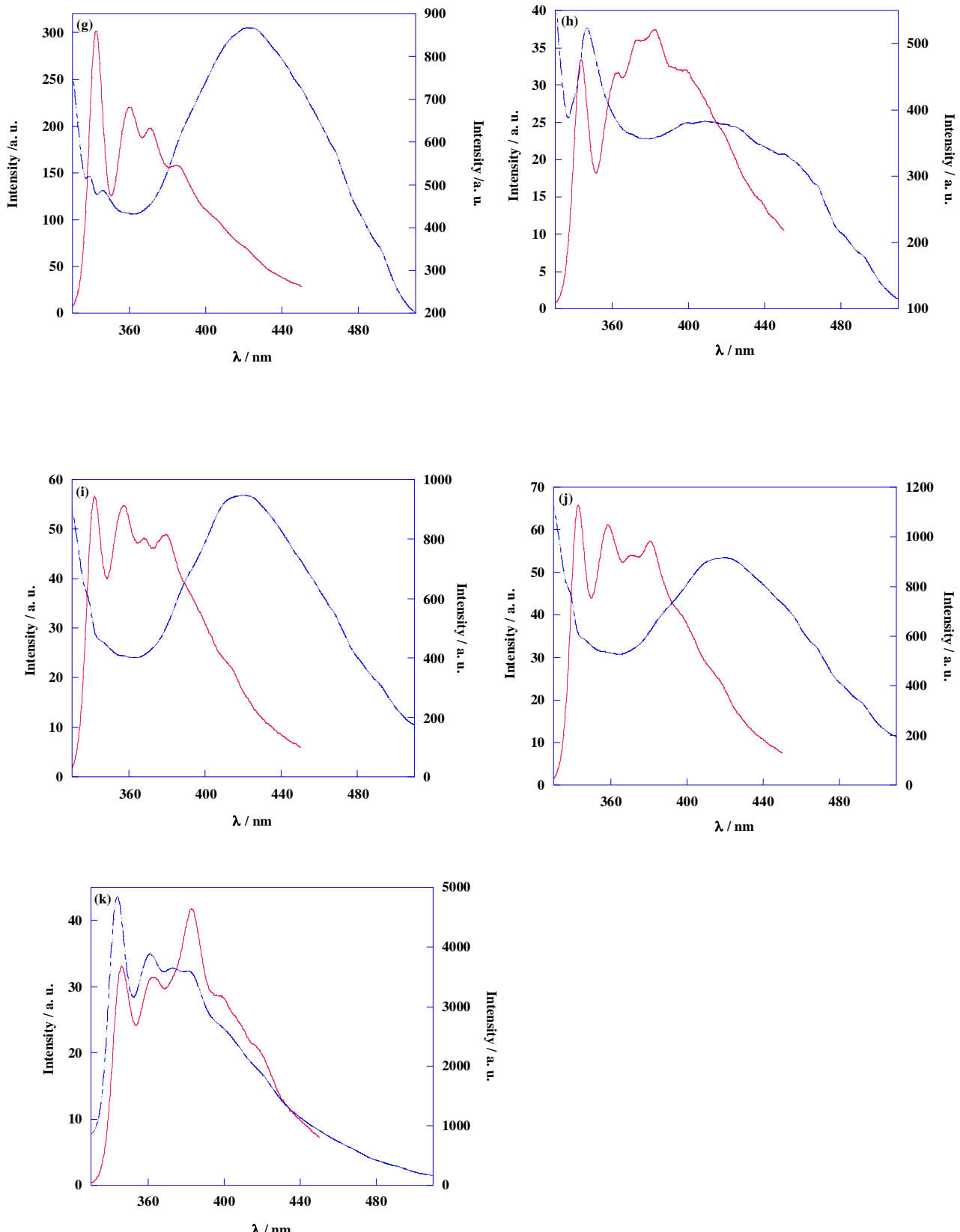


Fig. S10 Fluorescence spectra in solution (red line) and in solid state (blue line) corresponding to: (a) $[p\text{-C}_8\text{Br}_2]$ in ACN; (b) $[p\text{-C}_8\text{Br}_2]$ in THF; (c) $[p\text{-C}_{12}\text{Br}_2]$ in 1-PrOH; (d) $[p\text{-C}_{12}\text{Br}_2]$ in 2-PrOH; (e) $[p\text{-C}_{12}\text{Br}_2]$ in CHCl_3 ; (f) $[p\text{-C}_8(\text{NTf}_2)_2]$ in 2-PrOH; (g) $[p\text{-C}_8(\text{NTf}_2)_2]$ in CHCl_3 ; (h) $[p\text{-C}_8(\text{NTf}_2)_2]$ in 1,4-Diox; (i) $[p\text{-C}_{12}(\text{NTf}_2)_2]$ in ACN; (j) $[p\text{-C}_{12}(\text{NTf}_2)_2]$ in 1-PrOH; (k) $[p\text{-C}_{12}(\text{NTf}_2)_2]$ in THF.

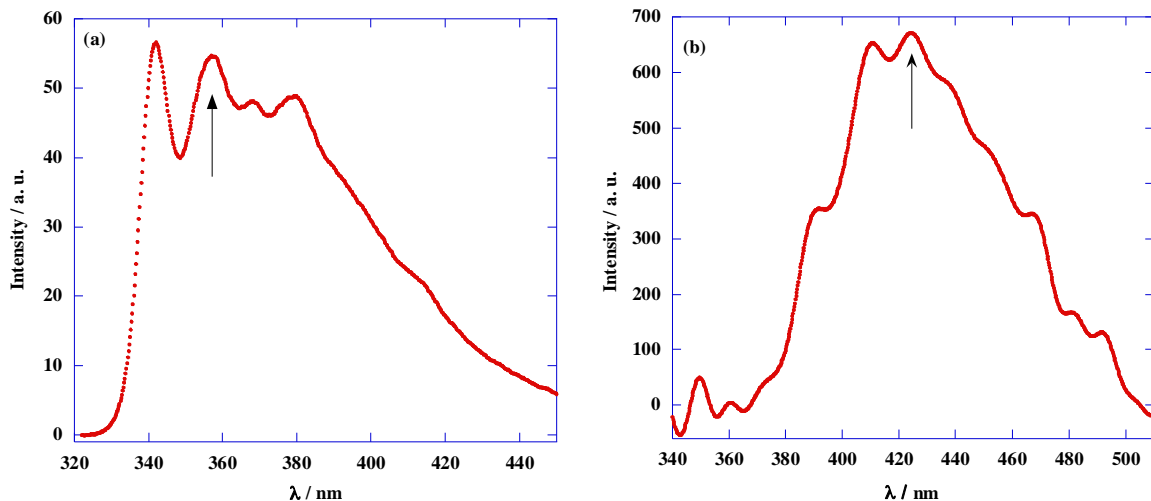


Fig. S11 (a) Solution and (b) deconvoluted solid state spectra for $[p\text{-C}_{12}\text{(NTf}_2)_2]$.

Table S1 RLS Intensity at 378 nm as function of salt and solvent nature ($[\text{salt}] = 1 \cdot 10^{-4}$ M).

Salt	Solvent	$I_{\text{RLS} \text{ 378 nm}}$
$[p\text{-C}_8\text{Br}_2]$	ACN	355
	THF	348
$[p\text{-C}_{12}\text{Br}_2]$	1-PrOH	500
	2-PrOH	514
$[p\text{-C}_8\text{(NTf}_2)_2]$	CHCl_3	576
	2-PrOH	540
	CHCl_3	440
$[p\text{-C}_{12}\text{(NTf}_2)_2]$	1,4-Diox	380
	ACN	480
	1-PrOH	504
	THF	565

Table S2 Estimated size of solvent molecules on the base of DFT geometries and AMBER atomic radii

Solvent	CAC	a	b	c	m/M
CHCl_3	0.82	10.0	10.0	4.8	0.48
2-PrOH	1.14	5.8	5.8	3.1	0.53
1,4-Diox	1.33	6.8	6.8	4.0	0.59
THF	1.44	6.0	6.0	4.0	0.67
1-PrOH	1.54	7.5	4.0	4.0	0.53
ACN	2.00	5.8	2.1	2.1	0.36

a,b and c are dimensions defining ellipsoid shape: $a=b>c$ for a oblate ellipsoid, $a>b=c$ for a prolate ellipsoid; m/M is the ratio between the minor and the major axis.

Table S3 λ_{MAX} and $\Delta\lambda$ values detected for fluorescence spectra recorded in solution and solid state at $1 \cdot 10^{-4}$ M.

Salt	Solvent	$\lambda_{\text{Solution}}/\text{nm}$	$\lambda_{\text{Solid State}}/\text{nm}$	$\Delta\lambda/\text{nm}$
$[p\text{-C}_8\text{Br}_2]$	ACN	358	434	76
	THF	362	395	33
$[p\text{-C}_{12}\text{Br}_2]$	1-PrOH	358	424	66
	2-PrOH	358	421	63
	CHCl_3	360	406	46
$[p\text{-C}_8(\text{NTf}_2)_2]$	2-PrOH	359	422	63
	CHCl_3	360	425	65
	1,4-Diox	362	413	51
$[p\text{-C}_{12}(\text{NTf}_2)_2]$	ACN	358	418	60
	1-PrOH	357	419	62
	THF	362	374	12